Thesis for the Degree of Master of Science

Synthesis of Polymer Nanocomposites *via* Activators ReGenerated by Electron Transfer Atom Transfer Radical Polymerization and Click Chemistry

By

Mai Thanh Binh

Department of Image System Engineering

The Graduate School

Pukyong National University

August 2013

Synthesis of Polymer Nanocomposites *via* Activators ReGenerated by Electron Transfer Atom Radical Transfer Polymerization and Click Chemistry

(ARGET ATRP 와 클릭화학을 이용한 고분자 나노컴포지트의 합성)

Advisor: Prof. Kwon Taek Lim

By

Mai Thanh Binh

A thesis submitted in partial fulfillment of the requirements

for the degree of

Master of Science

In Department of Image System Engineering, The Graduate School,

Pukyong National University

August 2013

Synthesis of Polymer Nanocomposites *via* Activators ReGenerated by Electron Transfer Atom Radical Transfer Polymerization and Click Chemistry

A dissertation

By

Mai Thanh Binh

Approved by:

Hoon Heo, Ph.D. (Chairman)

Jong Tae Kim, Ph.D. (Member)

Kwon Taek Lim, Ph.D. (Member)

August 2013

Dedicated to My Loving Parents

Mai Van Nguyen

And

Le Thi Dinh

Synthesis of Polymer Nanocomposites *via* Activators ReGenerated by Electron Transfer Atom Transfer Radical Polymerization and Click Chemistry

Mai Thanh Binh

Department of Image Science and Engineering, the Graduate School,
Pukyong National University

Abstract

Surface-initiated Atom Transfer Radical Polymerization (SI-ATRP) is an attractive method for synthesis of functional polymeric nanocomposites. However, the conventional SI-ATRP suffers two notorious drawbacks including large amount of metal catalyst and oxygen sensitivity of polymerization vessels. In this dissertation, a simple and greener synthesis of silica poly(methylmethacrylate) (SiO_2-PMMA) nanocomposites based on Activators ReGenerated by Electron Transfer Atom Transfer Radical Polymerization (ARGET ATRP) was reported. The formation of polymer chains covalently attached to silica surface was achieved via surface-initiated ARGET ATRP with using part per million (ppm) level of catalyst. In addition, a facile route for synthesis of thermo-responsive SiO_2-PNIPAm nanocomposites by combination of fascinating ARGET ATRP and click chemistry was also discussed. It was found that the surface of SiO_2 nanoparticles was tailored to be thermo-responsive upon the modification. ARGET ATRP is expected to provide a new and efficient method for synthesis of functional nanocomposites by both of “Grafting from” and “Grafting to” approaches.

ARGET ATRP와 클릭화학을 이용한 고분자 나노컴포지트의 합성

Mai Thanh Binh

부경대학교 대학원 이미지시스템공학과

요약

Surface-initiated Atom Transfer Radical Polymerization (SI-ATRP)는 기능성 고분자인 나노 복합 재료 합성방법으로 관심 받고 있다. 그러나 기존 SI-ATRP는 금속 촉매의 양이 많이 필요하다는 것과 중합 vessels의 산소 감도 등 두 가지 큰 단점을 가지고 있다. 이 논문에서, Activators ReGenerated by Electron Transfer Atom Transfer Radical Polymerization (ARGET ATRP)를 기초로 한 실리카 폴리(methyl methacrylate) (SiO_2-PMMA) 나노 복합 재료의 간단하고 친환경적인 합성방법을 보고한다. 실리카표면에 부착된 공유결합 고분자 형성은 촉매의 수준인 part per million(ppm) 을 사용하여 표면 개시된 ARGET ATRP를 통해 얻었다. 또한, ARGET ATRP 조합으로 열반응인 SiO_2-PNIPAm 나노 복합 재료의 합성에 손쉬운 경로와 click chemistry 대해서 논의 되었다. 이것은 SiO2 나노 입자의 표면이 수많은 수정된 열 반응으로 맞춰진 것으로 나타났다. ARGET ATRP는 "Grafting from"과 “Grafting to"의 접근으로써 기능성 나노 복합 재료의 합성을 위한 새로운 효과적인 방법을 제공 할 것으로 예상된다.

Table of contents

List of figures and tables

Chapter 1

General introduction

1.1. Introduction to polymeric nanocomposites

Polymer nanocomposites (PNC) consist of a polymer or copolymer having nanoparticles or nanofillers dispersed in the polymer matrix. These may be of different shape (platelets, fibers, spheroids), but at least one dimension must be in the range of 1–100 nm. These nanocomposites belong to the category of multi-phase systems (MPS) that consume nearly 95% of plastics production. These systems require controlled mixing/compounding, stabilization of the achieved dispersion, orientation of the dispersed phase, and the compounding strategies for all MPS, including PNC, are similar [1].

The transition from micro to nanoparticles leads to change in its physical as well as chemical properties [2]. Two of the major factors in this are the increase in the ratio of the surface area to volume, and the size of the particle. The increase in surface area to volume ratio, which increases as the particles get smaller, leads to an increasing dominance of the behavior of atoms on the surface area of particle over that of those interior of the particle. This affects the properties of the particles when they are reacting with other particles. Because of the higher surface area of the nanoparticles, the interaction with the other particles within the mixture is more and this increases the strength, heat resistance, etc. and many factors do change for the mixture. By combining organic substances with inorganic compounds, organic components can enhance the chemical stability and mechanical property [3, 4]That is to say, the desirable properties, which cannot be obtained when each component exists individually, can be achieved by the hybridization of organic and inorganic components [5, 6]. An example of a polymeric nanocomposites is silicon nanospheres which show quite different characteristics; in the size range of 40–100 nm, they are much harder than silicon, their hardness being between that of sapphire and diamond [7].

In recent years, a huge number of various nanocomposites based polymer with superior properties has been synthesized and applied for diverse fields such as high impact resistant materials, biomaterials, catalysts, and advanced opto-electronic devices [8-12].

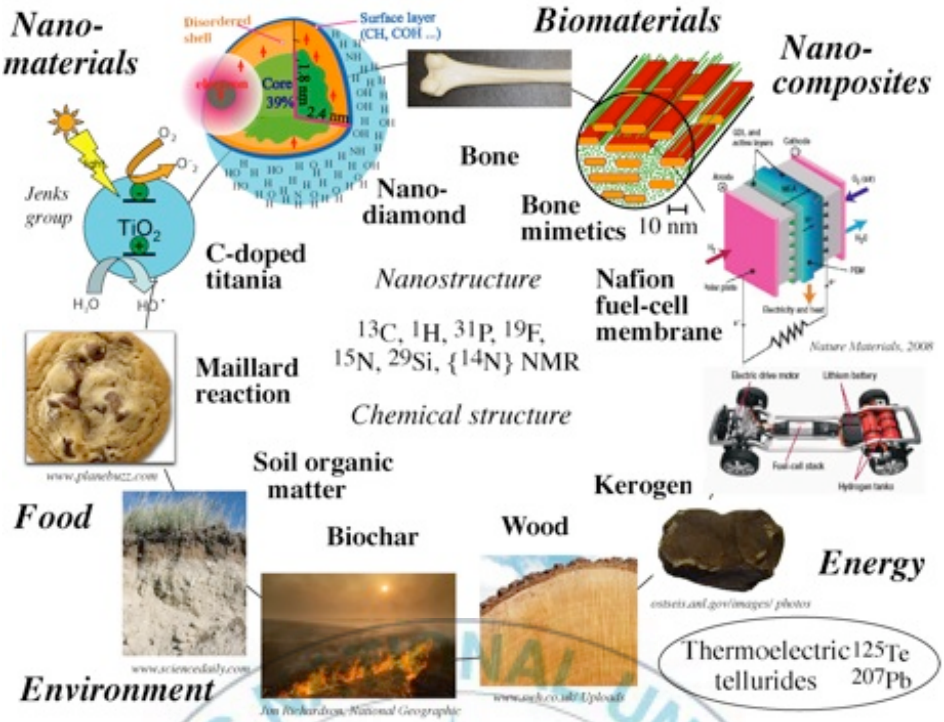

Figure 1.1. Applications of polymer nanocomposites.

1.2. Atom Transfer Radical Polymerization

Since first independently discovered by Krzysztof Matyjaszewsk [13] and by Mitsuo Sawamoto [14] in 1995, Atom Transfer Radical Polymerization (ATRP) has been one of the most effective and most widely used methods of controlled radical polymerization (CRP). ATRP is mechanistically related to transition metal mediated atom transfer radical addition (ATRA) reactions [15] and indeed this relationship was the reason this transition metal mediated controlled radical polymerization process was named ATRP [13]. ATRP can be viewed as a very special case of ATRA. However, in contrast to ATRA reactions, ATRP requires reactivation of the first formed alkyl halide adduct with the unsaturated compound (monomer) and the further reaction of the intermittently formed radical with additional monomer units (propagation) [16].

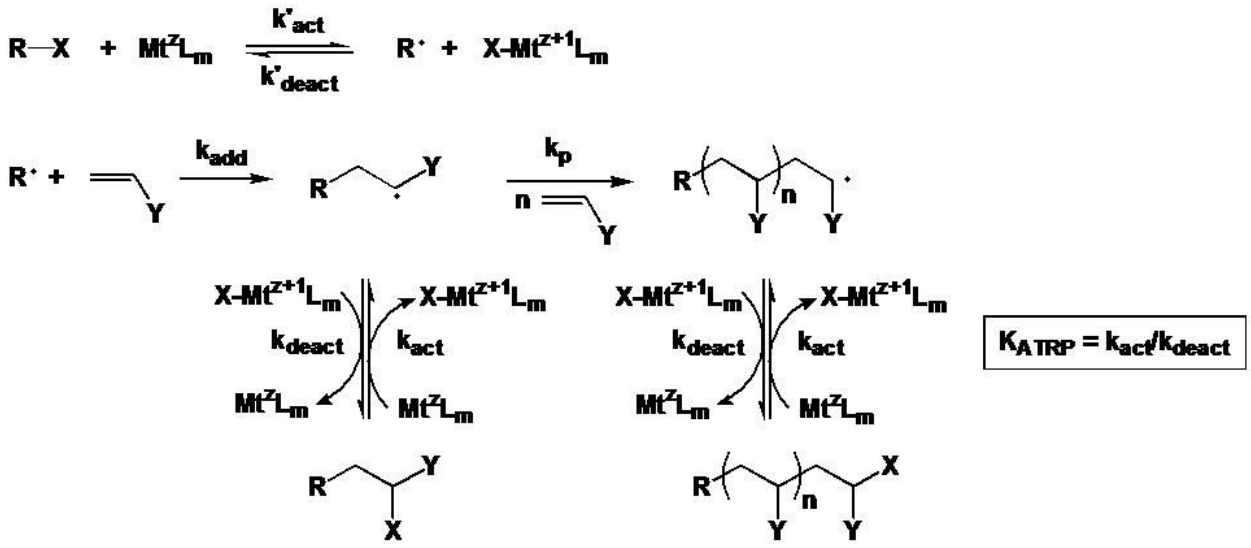

Figure 1.2. Mechanism of metal complex-mediated ATRA and ATRP [16].

The normal schematic of the ATRP equilibrium, which emphasizes the repetitive nature of the activation and deactivation steps and the need to push the equilibrium to the left hand side, thereby forming a low concentration of radicals to reduce radical-radical termination reactions, and ensure a high mole fraction of dormant chains, is shown below.

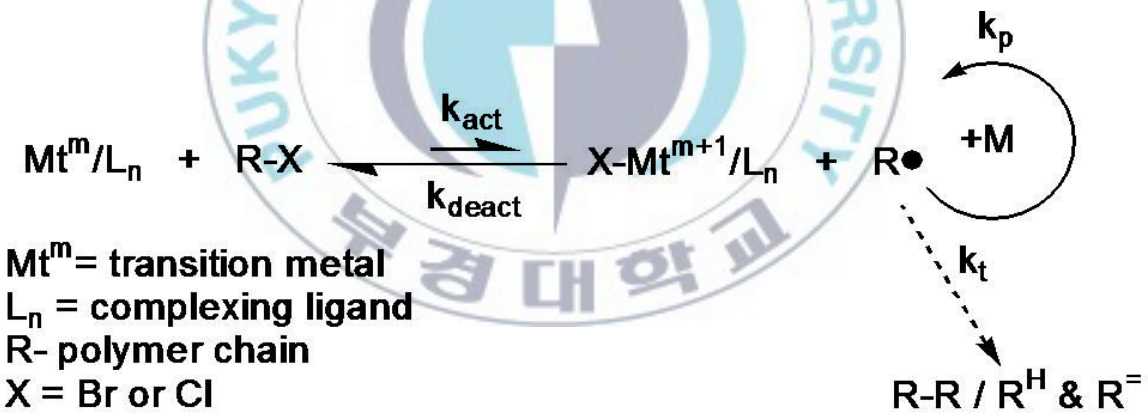

Figure 1.3. Mechanism of metal complex-mediated ATRP.

The "livingness" of this polymerization process can be ascertained from a linear first-order kinetic plot, accompanied by a linear increase in polymer molecular weight with conversion, with the value of the number-average degree of polymerization (DP_n) determined by the ratio of reacted monomer to initially introduced initiator ($DP_n = D[M]/[RX]_0$).

ATRP is based on an inner sphere electron transfer process [17], which involves a reversible homolytic (pseudo) halogen transfer between a dormant species, an added initiator or dormant propagating chain end (R-X or R-P_n-X) and a transition metal complex in the lower oxidation state

(Mt^m/L_n), resulting in the formation of propagating radicals ($R^\bullet$) [18] and the metal complex in the higher oxidation state with a coordinated halide ligand ($X\text{-}Mt^{m+1}/L_n$). The active radicals form with a measurable rate constant of activation k_{act}, subsequently propagate with a rate constant k_p and are reversibly deactivated k_{deact}, but, since ATRP is a radical based process, the active species can also terminate with a rate constant k_t. As the reaction progresses radical termination is diminished as a result of the persistent radical effect (PRE) [8, 19, 20], increased chain length, as well as conversion and viscosity [21]. Consequently, the equilibrium is strongly shifted towards the dormant species ($k_{act} << k_{deact}$) [20].

ATRP is a particularly successful CRP that has attracted commercial interests because ATRP reactions are tolerant of various functional groups such as allyl [22], amino [23], epoxy [24], hydroxy [25] and vinyl exist in either the monomer or the initiator [26]. Moreover, ATRP reactions also possess easy experimental setup, use of readily accessible and inexpensive catalyst components, usually copper complexes formed with commercially available aliphatic amines, imines, or pyridine based ligands, and simple commercially available or easily prepared initiators or macro-initiators (often alkyl halides) [27].

1.3. Activators ReGenerated by Electron Transfer (ARGET) Atom Transfer Radical Polymerization

Although ATRP has proved to be the most popular CRP technology for the formation of several well-defined polymers as well as polymeric nanocomposites, the conventional ATRP still suffers two notorious drawbacks, including high sensitive procedure requiring stringent reaction conditions, such as the limitation of no air and the use of high concentrations of copper catalyst leading to polymer contamination [27]. Therefore, an immense research interest has been proceeded in order to gain a milder polymerization process based ATRP without defection of control manner. In recent years, Matyjaszewski and co-workers first described controlled radical polymerization by Activators ReGenerated by Electron Transfer Atom Transfer Radical Polymerization (ARGET ATRP) [28-30], a development of the very widely used ATRP technology. ARGET ATRP offers two principle advantages over conventional ATRP: improved tolerance of oxygen and significantly reduced heavy metal catalyst concentrations. Therefore, ARGET ATRP provides a powerful method for preparation of various polymer based materials. Several homopolymers, block copolymers as well as polymeric nanocomposites with well-controlled structures and composition have been successfully synthesized via this facile route [31-34].

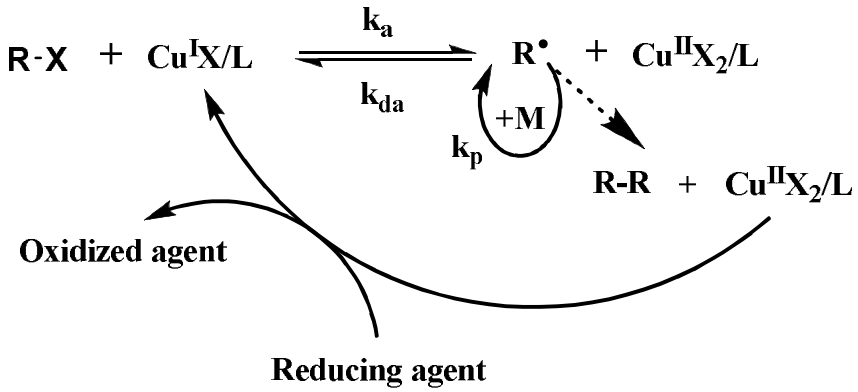

Figure 1.4. Mechanism of ARGET ATRP.

1.4. Click chemistry

Current advances in our understanding of molecular biology, microelectronics, and sensorics have fueled increasing needs for materials with more sharply defined structures [35]; however, the preparation of such materials imposes major synthetic challenges. In fact, many of the currently used processes to synthesize materials allow only crude control over the structure of the material. As a consequence, man-made materials often do not match the superb properties of natural materials such as proteins, DNA, or sugars [36]. To address this gap between the sophisticated functionality that is required for future advances in bio- and nanotechnology and the limited chemical control offered by many of the synthetic materials processes that are currently available, we are now witnessing an increasing infusion of synthetic organic chemistry concepts into materials science [37]. This trend appears to be motivated by the prospect of molecular-level control during the preparation of nanostructured materials. In spite of the evident differences between small molecules and macromolecules, attempts to extend synthetic concepts from organic chemistry into the nanometer- and mesoscale dimensions have been increasingly fruitful [37]. For a synthetic organic concept to be applicable to the preparation of macromolecules, the reactions must i) result in a stable linkage, ii) exhibit minimal cross-reactivity with other functional groups, iii) react to completion, iv) be free of appreciable amounts of side products, and v) proceed under benign reaction conditions [38].

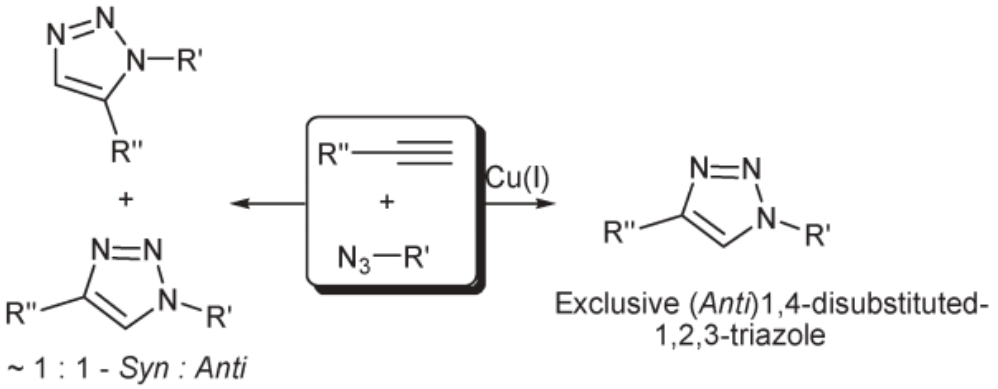

Figure 1.5. 1,3-dipolar cycloaddition of alkyne and azide.

Sharpless and others have recently developed a framework of reactions that is often referred to as “click chemistry”. This synthetic framework, which fulfills all of the above-mentioned criteria, may have great potential for use in the synthesis of materials. As such, click reactions are driven by a high thermodynamic force (> 20 kcal mol^{-1}), which gives rise to highly modular and stereospecific reactions with high yields. In that sense, click chemistry is not limited to a specific type of reaction (e.g., Friedel–Crafts acylation or Baeyer–Villiger oxidation) but rather defines a synthetic concept or framework that comprises a range of reactions, with different reaction mechanisms, but common reaction trajectories. In fact, Sharpless defined click chemistry early on as the generation of complex substances by bringing together smaller units via heteroatoms. While a range of chemical reactions can in principle fulfill these criteria, successful examples often originate from five broad classes of reactions that appear to fit the framework of click chemistry exceptionally well [39]:

1. Cycloaddition of unsaturated species: 1,3-dipolar cycloaddition.
2. Cycloaddition of unsaturated species: [4+2]-cycloaddition (Diels–Alder).
3. Nucleophilic substitution/ring-opening reactions.
4. Carbonyl reactions of the non-aldol type.
5. Addition to carbon–carbon multiple bonds.

The reaction of thiols with enes, whether proceeding by a radical (termed thiol–ene reaction) or anionic chain (termed thiol Michael addition), carry many of the attributes of click reactions [40]. These attributes include achieving quantitative yields, requiring only small concentrations of relatively benign catalysts, having rapid reaction rates with reactions occurring either in bulk or in environmentally benign solvents over a large concentration range, requiring essentially no clean up,

being insensitive to ambient oxygen or water, yielding a single regioselective product, and the ready availability of an enormous range of both thiols and enes [41]. This exceptional versatility and its propensity for proceeding to quantitative conversions under even the mildest of conditions makes thiol–ene chemistry amenable to applications ranging from high performance protective polymer networks to processes that are important in the optical, biomedical, sensing, and bioorganic modification fields [42]. Accordingly, both the thiol–ene radical and thiol Michael addition reactions are now routinely referred to in the literature as thiol click reactions.

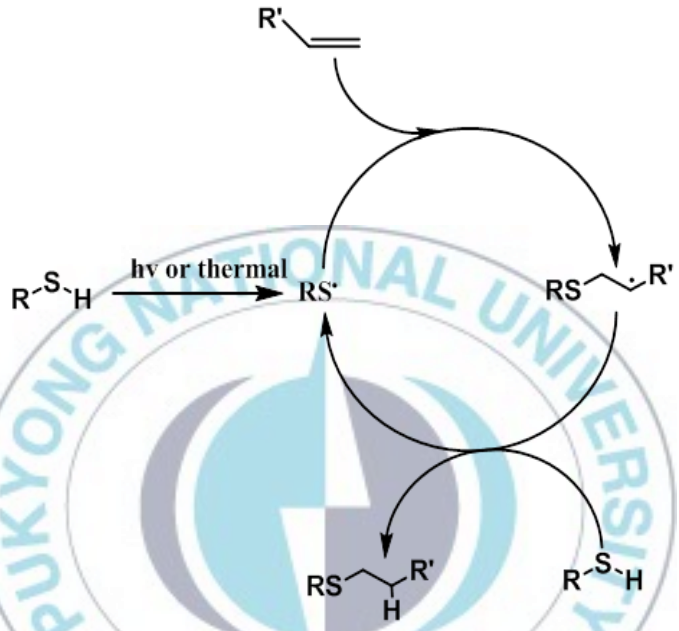

Figure 1.6. Thiol-ene addition of thiol and alkene.

The chemistry of thiols, whether radical- or catalyst-mediated, is certainly influenced by the basic structure of the thiol. Four prominent thiol types typically encountered in literature reports include alkyl thiols, thiophenols, thiol propionates, and thiol glycolates [43]. Both types of thiol click reaction are extremely efficient; radical addition has been known to proceed by an efficient step-growth chain process for several decades [43]. There have been several reviews of thiol–ene radical chemistry and polymerization, the latest being in 2004. By 2004, it had been plainly and extensively demonstrated that thiol–ene networks serve as benchmark polymer materials that can react to form highly uniform glasses, elastomers, and adhesives [44]. Any non-sterically hindered terminal ene is capable of participating in the radical-mediated thiol–ene process, with electron-rich (vinyl ether) and/or strained enes (norbornene) reacting more rapidly than electron-deficient enes. Cross-linked polymers formed from these systems are the most ideal homogeneous network

structures ever formed by free-radical polymerization, with narrow glass transition regions and extremely low polymerization shrinkage stress [40, 45].

1.5. Silica-polymer nanocomposites

Organic/inorganic composite materials have been extensively studied for a long time. When inorganic phases in organic/inorganic composites become nanosized, they are called nanocomposites. Organic/inorganic nanocomposites are generally organic polymer composites with inorganic nanoscale building blocks. They combine the advantages of the inorganic material (e.g., rigidity, thermal stability) and the organic polymer (e.g., flexibility, dielectric, ductility, and processability). Moreover, they usually also contain special properties of nanofillers leading to materials with improved properties. A defining feature of polymer nanocomposites is that the small size of the fillers leads to a dramatic increase in interfacial area as compared with traditional composites. This interfacial area creates a significant volume fraction of interfacial polymer with properties different from the bulk polymer even at low loadings [1, 46-50]. Inorganic nanoscale building blocks include nanotubes, layered silicates (e.g., montmorillonite, saponite), nanoparticles of metals (e.g., Au, Ag), metal oxides (e.g., TiO_2, Al_2O_3), semiconductors (e.g., PbS, CdS), and so forth, among which SiO_2 is viewed as being very important. Therefore, polymer/silica nanocomposites have attracted substantial academic and industrial interest. In fact, among the numerous inorganic/organic nanocomposites, polymer/silica composites are the most commonly reported in the literature. They have received much attention in recent years and have been employed in a variety of applications. As pointed out by Hajji et al. [51], nanocomposite systems can be prepared by various synthesis routes, thanks to the ability to combine different ways to introduce each phase. The organic component can be introduced as (i) a precursor, which can be a monomer or an oligomer, (ii) a preformed linear polymer (in molten, solution, or emulsion states), or (iii) a polymer network, physically (e.g., semicrystalline linear polymer) or chemically (e.g., thermosets, elastomers) cross-linked. The mineral part can be introduced as (i) a precursor (e.g., TEOS) or (ii) preformed nanoparticles.

Organic or inorganic polymerization generally becomes necessary if at least one of the starting moieties is a precursor. This leads to three general methods for the preparation of polymer/silica nanocomposites according to the starting materials and processing techniques: blending, sol-gel processes, and in situ polymerization (Scheme 1). Blending is generally just mixing of the silica nanoparticles into the polymer; a sol-gel process can be done in situ in the presence of a preformed

organic polymer or simultaneously during the polymerization of the monomer(s); the method of in situ polymerization involves the dispersion of nanosilica in the monomer(s) first and then polymerization is carried out. In addition, considerable efforts have been devoted to the design and controlled fabrication of polymer/silica colloidal nanocomposite particles with tailored morphologies in recent years. The colloids represent a relatively new category of nanocomposites.

The preparation, characterization, properties, and applications of polymer/silica nanocomposites have become a quickly expanding field of research. A key feature in the construction of nanocomposite systems is the development of specific interactions at the interface of the organic and inorganic components, because the interface plays a dominant role in the preparation and properties of nanocomposites. Therefore, the development of grafting strategies so as to tailor the surface properties of mineral substrates is of great current interest. As mentioned above, two general routes have been used to graft linear polymer chains at the surface of the particles. One method is the "grafting-to" technique and the other method is the "grafting-from" technique.

The grafting of polymers to inorganic particles such as silica is effective at improving the surface, but contamination from nongrafted chains usually occurs. Then separation of the grafted chains from the nongrafted ones remains difficult. Also, strong hindrance between grafted polymer chains prevents attachment of further ones and then limits the graft density.

The "grafting-from" technique, also called surface-initiated polymerization, for example, polymerization performed in situ with monomer growth of polymer chains from immobilized initiators on mineral surfaces, leading to the formation of so-called "polymer brushes" or "hairy nanoparticles", appears to be a very promising and versatile method. A large variety of initiating mechanisms, including free radical polymerization, which involves conventional radical polymerizations [52-56] and controlled radical polymerization (CRP) [57-63], living anionic polymerization [64], living cationic polymerization [65-67], ring opening polymerization (ROP) [68, 69], ring opening metathesis polymerization (ROMP) [70, 71], and others [72, 73], have been applied.

Among them, controlled CRP has become the most popular route, which is usually divided into three categories: atom transfer radical polymerization (ATRP) [23, 58, 60], nitroxide mediated polymerization (NMP, also referred to as stable free-radical polymerization) [74, 75], and reversible radical addition, fragmentation, and transfer (RAFT) polymerization [76-78]. All three techniques

permit the polymer molecular weight, the polydispersity, and the polymer architecture to be accurately controlled.

Since the polymer/silica nanocomposites not only can improve the physical properties such as the mechanical properties and thermal properties of the materials, but can also exhibit some unique properties, they have attracted strong interest in many industries. Besides common plastics and rubber reinforcement, many other potential and practical applications of this type of nanocomposite have been reported: coatings [79, 80], flame-retardant materials [81, 82], optical devices [83, 84] electronics and optical packaging materials [85, 86] photoresist- materials [87, 88], photo-luminescent conducting film [89], pervaporation membrane [90, 91], ultra-permeable reverse-selective membranes [92], proton exchange membranes [93], grouting materials [94], sensors [95], materials for metal uptake [96], etc. As for the colloidal polymer/silica nanocomposites with various morphologies, they usually exhibit enhanced, even novel, properties compared with the traditional nanocomposites and have many potential applications in various areas such as coatings, catalysis, and biotechnologies.

1.6. Aim of this thesis

The aim of this thesis is to develop facile routes for preparation of polymer-inorganic nanocomposites by the utilization of controlled radical polymerization (ARGET ATRP) and click chemistry via both of grafting from and grafting to approach.

In the first part of this thesis, surface-initiated ARGET ATRP was used for synthesis of SiO2-PMMA nanocomposites. The surface-initiated polymerization of nanocomposites was achieved by employing Copper(II)/Tin (II) hexanoate (Catalyst/Reducing agent) in anisole under mild condition (without elevated temperature). It was found that the grafting density of PMMA onto silica surface could be well-controlled by controlling of reaction time.

Moreover, the surface modification of silica nanoparticles with thermo-responsive poly(N-isopropyl acrylamide) (PNIPAm) by combination of ARGET ATRP and thiol-ene chemistry was also discussed. The well-defined PNIPAm was prepared by fascinating ARGET ATRP with ppm level of copper catalyst and subsequently immobilized onto silica surface by high efficient thiol-ene click reaction. Upon the modification, it was demonstrated that the surface of silica had been tailored with thermo-responsive properties of the polymer. The as-synthesized nanocomposites with thermo-responsive behavior may be found for application in biotechnology area.

1.7. Reference

1. L. S. Schadler, *Polymer-Based and Polymer-Filled Nanocomposites*, in *Nanocomposite Science and Technology*, Wiley-VCH Verlag GmbH & Co. KGaA **(2004)**.

2. P. M. Ajayan, *Bulk Metal and Ceramics Nanocomposites*, in *Nanocomposite Science and Technology*, Wiley-VCH Verlag GmbH & Co. KGaA **(2004)**.

3. X. Ji, J. E. Hampsey, Q. Hu, *Chemistry of Materials* 15, 3656 **(2003)**.

4. H. Peng, J. Tang, L. Yang, *Journal of the American Chemical Society* 128, 5304 **(2006)**.

5. S. Bandi, M. Bell, and D. A. Schiraldi, *Macromolecules* 38, 9216 **(2005)**.

6. A. Pich, S. Bhattacharya, Y. Lu, *Langmuir* 20, 10706 **(2004)**.

7. H. Zou, S. Wu, and J. Shen, *Chemical Reviews* 108, 3893 **(2008)**.

8. H. K. Joseph, *Current Status, Trends, Future Directions, and Opportunities*, in *Polymer Nanocomposites: Processing, Characterization, and Applications*, McGraw Hill Professional, Access Engineering **(2006)**.

9. H. K. Joseph, *Processing of Nanomaterials*, in *Polymer Nanocomposites: Processing, Characterization, and Applications*, McGraw Hill Professional, Access Engineering **(2006)**.

10. D. Kim, S. Srivastava, S. Narayanan, *Soft Matter* 8, 10813 **(2012)**.

11. H. Kim, A. A. Abdala, and C. W. Macosko, *Macromolecules* 43, 6515 **(2010)**.

12. N. G. Sahoo, S. Rana, J. W. Cho, *Progress in Polymer Science* 35, 837 **(2010)**.

13. J.-S. Wang and K. Matyjaszewski, *Journal of the American Chemical Society* 117, 5614 **(1995)**.

14. M. Kato, M. Kamigaito, M. Sawamoto, *Macromolecules* 28, 1721 **(1995)**.

15. F. Minisci, *Accounts of Chemical Research* 8, 165 **(1975)**.

16. T. Pintauer and K. Matyjaszewski, *Chemical Society Reviews* 37, 1087 **(2008)**.

17. K. Matyjaszewski, *Macromolecular Symposia* 134, 105 **(1998)**.

18. D. A. Singleton, D. T. Nowlan, N. Jahed, *Macromolecules* 36, 8609 **(2003)**.

19. H. Fischer, *Chemical Reviews* 101, 3581 **(2001)**.

20. W. Tang, N. V. Tsarevsky, and K. Matyjaszewski, *Journal of the American Chemical Society* 128, 1598 **(2006)**.

21. P. Vana, T. P. Davis, and C. Barner-Kowollik, *Macromolecular Rapid Communications* 23, 952 **(2002)**.

22. R. París and J. L. de la Fuente, *Journal of Polymer Science Part A: Polymer Chemistry* 43, 2395 **(2005)**.

23. S. B. Lee, A. J. Russell, and K. Matyjaszewski, *Biomacromolecules* 4, 1386 **(2003)**.

24. P. F. Cañamero, J. L. de la Fuente, E. L. Madruga, *Macromolecular Chemistry and Physics* 205, 2221 **(2004)**.

25. K. L. Robinson, M. A. Khan, M. V. de Paz Báñez, *Macromolecules* 34, 3155 **(2001)**.

26. U. Mansfeld, C. Pietsch, R. Hoogenboom, *Polymer Chemistry* 1, 1560 **(2010)**.

27. K. Matyjaszewski, *Macromolecules* 45, 4015 **(2012)**.

28. W. Jakubowski, K. Min, and K. Matyjaszewski, *Macromolecules* 39, 39 **(2005)**.

29. W. Jakubowski and K. Matyjaszewski, *Angewandte Chemie* 118, 4594 **(2006)**.

30. K. Matyjaszewski, W. Jakubowski, K. Min, *Proceedings of the National Academy of Sciences* 103, 15309 **(2006)**.

31. S. Hansson, E. Östmark, A. Carlmark, *ACS Applied Materials & Interfaces* 1, 2651 **(2009)**.

32. L. Mueller, W. Jakubowski, W. Tang, *Macromolecules* 40, 6464 **(2007)**.

33. H. Chen, L. Yang, Y. Liang, *Journal of Polymer Science Part A: Polymer Chemistry* 47, 3202 **(2009)**.

34. P. Shivapooja, L. Ista, H. Canavan, *Biointerphases* 7, 1 **(2012)**.

35. J. E. Moses and A. D. Moorhouse, *Chemical Society Reviews* 36, 1249 **(2007)**.

36. Y. Hua and A. H. Flood, *Chemical Society Reviews* 39, 1262 **(2010)**.

37. J. E. Hein and V. V. Fokin, *Chemical Society Reviews* 39, 1302 **(2010)**.

38. C. O. Kappe and E. Van der Eycken, *Chemical Society Reviews* 39, 1280 **(2010)**.

39. H. Nandivada, X. Jiang, and J. Lahann, *Advanced Materials* 19, 2197 **(2007)**.

40. C. E. Hoyle and C. N. Bowman, *Angewandte Chemie International Edition* 49, 1540 **(2010)**.

41. C. R. Morgan, F. Magnotta, and A. D. Ketley, *Journal of Polymer Science: Polymer Chemistry Edition* 15, 627 **(1977)**.

42. *Journal of the Society of Chemical Industry* 57, 752 **(1938)**.

43. K. Griesbaum, *Angewandte Chemie* 82, 276 **(1970)**.

44. C. E. Hoyle, T. Y. Lee, and T. Roper, *Journal of Polymer Science Part A: Polymer Chemistry* 42, 5301 **(2004)**.

45. P. Thirumurugan, D. Matosiuk, and K. Jozwiak, *Chemical Reviews* **(2013)**.

46. A. C. Balazs, T. Emrick, and T. P. Russell, *Science* 314, 1107 **(2006)**.

47. K. I. Winey and R. A. Vaia, *MRS Bulletin* 32, 314 **(2007)**.

48. R. Krishnamoorti and R. A. Vaia, *Journal of Polymer Science Part B: Polymer Physics* 45, 3252 **(2007)**.

49. L. S. Schadler, S. K. Kumar, B. C. Benicewicz, *MRS Bulletin* 32, 335 **(2007)**.

50. D. W. Schaefer and R. S. Justice, *Macromolecules* 40, 8501 **(2007)**.

51. P. Hajji, L. David, J. F. Gerard, *Journal of Polymer Science Part B: Polymer Physics* 37, 3172 **(1999)**.

52. Y. Shirai and N. Tsubokawa, *Reactive and Functional Polymers* 32, 153 **(1997)**.

53. Y. Noishiki, Y. Nishiyama, M. Wada, *Journal of Applied Polymer Science* 86, 3425 **(2002)**.

54. R. Yokoyama, S. Suzuki, K. Shirai, *European Polymer Journal* 42, 3221 **(2006)**.

55. M. Satoh, K. Shirai, H. Saitoh, *Journal of Polymer Science Part A: Polymer Chemistry* 43, 600 **(2005)**.

56. Y. Taniguchi, K. Shirai, H. Saitoh, *Polymer* 46, 2541 **(2005)**.

57. C. R. Vestal and Z. J. Zhang, *Journal of the American Chemical Society* 124, 14312 **(2002)**.

58. Y. Wang, X. Teng, J.-S. Wang, *Nano Letters* 3, 789 **(2003)**.

59. P. S. Chinthamanipeta, S. Kobukata, H. Nakata, *Polymer* 49, 5636 **(2008)**.

60. C. Perruchot, M. A. Khan, A. Kamitsi, *Langmuir* 17, 4479 **(2001)**.

61. Z. Wei, M. Wan, T. Lin, *Advanced Materials* 15, 136 **(2003)**.

62. C.-D. Vo, A. Schmid, S. P. Armes, *Langmuir* 23, 408 **(2006)**.

63. A. El Harrak, G. Carrot, J. Oberdisse, *Macromolecules* 37, 6376 **(2004)**.

64. Q. Zhou, S. Wang, X. Fan, *Langmuir* 18, 3324 **(2002)**.

65. U. Eismann and S. Spange, *Macromolecules* 30, 3439 **(1997)**.

66. S. Höhne, A. Seifert, M. Friedrich, *Macromolecular Chemistry and Physics* 205, 1667 **(2004)**.

67. R. Zirbs, W. Binder, M. Gahleitner, *Macromolecular Symposia* 254, 93 **(2007)**.

68. G. Carrot, D. Rutot-Houzé, A. Pottier, *Macromolecules* 35, 8400 **(2002)**.

69. K. R. Yoon, Y.-W. Lee, J. K. Lee, *Macromolecular Rapid Communications* 25, 1510 **(2004)**.

70. A.-F. Mingotaud, S. Reculusa, C. Mingotaud, *Journal of Materials Chemistry* 13, 1920 **(2003)**.

71. M. A. Jordi and T. A. P. Seery, *Journal of the American Chemical Society* 127, 4416 **(2005)**.

72. Y.-P. Wang, X.-W. Pei, and K. Yuan, *Materials Letters* 59, 520 **(2005)**.

73. Y.-P. Wang, X.-W. Pei, X.-Y. He, *European Polymer Journal* 41, 1326 **(2005)**.

74. L. Sonnenberg, J. Parvole, O. Borisov, *Macromolecules* 39, 281 **(2005)**.

75. C. Bartholome, E. Beyou, E. Bourgeat-Lami, *Macromolecules* 36, 7946 **(2003)**.

76. C. Li and B. C. Benicewicz, *Macromolecules* 38, 5929 **(2005)**.

77. C. Li, J. Han, C. Y. Ryu, *Macromolecules* 39, 3175 **(2006)**.

78. Y. Zhao and S. Perrier, *Macromolecules* 40, 9116 **(2007)**.

79. F. Bauer, V. Sauerland, H. Ernst, *Macromolecular Chemistry and Physics* 204, 375 **(2003)**.

80. F. Bauer, H. Ernst, D. Hirsch, *Macromolecular Chemistry and Physics* 205, 1587 **(2004)**.

81. G. H. Hsiue, Y. L. Liu, and H. H. Liao, *Journal of Polymer Science Part A: Polymer Chemistry* 39, 986 **(2001)**.

82. C.-L. Chiang, C.-C. M. Ma, D.-L. Wu, *Journal of Polymer Science Part A: Polymer Chemistry* 41, 905 **(2003)**.

83. C.-C. Chang and W.-C. Chen, *Chemistry of Materials* 14, 4242 **(2002)**.

84. C. Z. Chuai, K. Almdal, and J. Lyngaae-Jørgensen, *Polymer* 44, 481 **(2003)**.

85. Y. Sun, Z. Zhang, and C. P. Wong, *Polymer* 46, 2297 **(2005)**.

86. Y. Sun, Z. Zhang, K.-S. Moon, *Journal of Polymer Science Part B: Polymer Physics* 42, 3849 **(2004)**.

87. J.-D. Cho, H.-T. Ju, Y.-S. Park, *Macromolecular Materials and Engineering* 291, 1155 **(2006)**.

88. I. Sondi, T. H. Fedynyshyn, R. Sinta, *Langmuir* 16, 9031 **(2000)**.

89. X. Li, X. Li, and G. Wang, *Materials Letters* 60, 3342 **(2006)**.

90. M. Khayet, J. P. G. Villaluenga, J. L. Valentin, *Polymer* 46, 9881 **(2005)**.

91. Y.-L. Liu, C.-Y. Hsu, Y.-H. Su, *Biomacromolecules* 6, 368 **(2004)**.

92. T. C. Merkel, B. D. Freeman, R. J. Spontak, *Science* 296, 519 **(2002)**.

93. Y.-H. Su, Y.-L. Liu, Y.-M. Sun, *Journal of Power Sources* 155, 111 **(2006)**.

94. X. J. Xiang, J. W. Qian, W. Y. Yang, *Journal of Applied Polymer Science* 100, 4333 **(2006)**.

95. Y.-l. Su, *Reactive and Functional Polymers* 66, 967 **(2006)**.

96. K. G. Neoh, K. K. Tan, P. L. Goh, *Polymer* 40, 887 **(1999)**.

Chapter 2

Facile synthesis of SiO_2-poly(methyl methacrylate) nanocomposites *via* surface-initiated ARGET ATRP

In this chapter, a facile route for covalent functionalization of silica (SiO_2) nanoparticles with poly(methyl methacrylate) (PMMA) has been disclosed. SiO_2 nanoparticles surface was treated with 2-bromo-2-methyl-N-3-[(trimethoxysilyl)propyl]-propan-amide (BrTMSPA) to introduce the initiator onto surface. Subsequently, a process called **A**ctivators **Re**g**e**nerated by **E**lectron **T**ransfer (ARGET) ATRP was employed for synthesis of SiO_2/PMMA nanocomposites with ppm level of copper catalyst. The success of modification was confirmed by surface analysis including Fourier-Transform Infrared (FT-IR) and Xray Photoelectron Spectroscopy (XPS). The morphology of nanocomposites was investigated by Field Emission Scanning Electron Microscope (FE-SEM) and Transmission Electron Microscope (TEM). Thermogravimetric analysis (TGA) was used to evaluate thermal properties and grafting density.

2.1. Introduction

The wide application of silica (SiO_2) composites in bone replacement and tissue engineering has been limited as a result of the poor distribution of SiO_2 additives in composites [1-3]. The most common method to overcome this problem is grafting polymer on the SiO_2 surface, which not only enhances the dispersion of SiO_2 but also increases the compatibility of SiO_2 with the polymer matrix [4-7]. Various methods have been developed to graft polymer onto the SiO_2 surface, for example, silane coupling agents [8, 9], organic isocyanates [10, 11] and ring opening polymerization [12, 13]. The amount of grafted polymer is an important factor for the ultimate mechanical strength of the composites. It has been reported that poly(l-lactic acid) (PLLA) grafted on the SiO_2 particles improved the tensile strength of the PLLA/SiO_2 composites [14] and poly(ε-caprolactone) (PCL) grafted improved the compressive strength of the PCL/SiO_2 composite scaffolds [14]. Moreover, many methods have been employed to decorate SiO_2 particles to increase the amount of grafted polymer, which significantly improved mechanical properties [1, 15-18].

The past decade has witnessed the explosive development of controlled/living radical polymerization (CRP) processes [19-21]. Macromolecules with precisely controlled architecture and functionality have been synthesized from a wide range of monomers under conditions that are much less rigorous than previously required for ionic living polymerizations [22-24]. In addition, a plethora of new functional materials have been prepared, including molecular composites, hybrids, and bio-conjugates [25-27]. Atom-transfer radical polymerization (ATRP) is among the most efficient and robust CRP processes [28-30]. ATRP is especially well-suited for surface modification, bio-conjugation, and the preparation of molecular brushes because hydroxyl or amine groups on the surface or in natural products can be easily converted to ATRP-active initiators: R-bromo-esters or R-bromo-amides. Matyjaszewski group and many others have shown how to control the growth of well-defined polymer chains from flat silicon wafers and also from various convex, concave, and irregular surfaces [31-34]. ATRP and essentially all CRP processes can be carried out in bulk, solution, or dispersed media (including aqueous systems) [32]. However, because propagating radicals are rapidly trapped by oxygen, reaction mixtures must be rigorously deoxygenated. Matyjaszewski group has previously demonstrated that in ATRP systems air can be consumed by adding a sufficient amount of an appropriate reducing agent, such as metallic copper, tin(II) 2-ethylhexanoate, which has been approved by the Food and Drug Administration (FDA), or ascorbic acid (vitamin C) in a process called activators generated by electron transfer (AGET) [35].

ATRP is based on the intermittent activation of alkyl halides to generate propagating radicals in the presence of redox-active transition-metal complexes, which are typically copper halides with polydentate N-based ligands. In AGET ATRP, the activator (Cu(I) species) is first rapidly oxidized by oxygen to the Cu(II) species, but the latter is quickly reduced to the Cu(I) state in the presence of a reducing agent. There is an induction period during which air is consumed, and eventually the polymerization starts. This process has been successfully used to prepare well-defined products in organic media and also in miniemulsion [36, 37]. Unfortunately, it is difficult to estimate the exact amount of reducing agent needed. If it is added in too large of an excess, then polymerization control is lost because nearly all of the deactivator (Cu (II) species) is consumed and a relatively large amount of Cu (I) activator leads to uncontrolled ATRP that is too fast. On the contrary, an insufficient amount of reducing agent does not consume all of the air and results in no polymerization. We have recently improved the AGET process by employing a very active copper catalyst used in minute amounts in the presence of excess reducing agent that reacts slowly. Under these conditions, activators are continuously regenerated by electron transfer (ARGET), and even parts per million amounts of catalysts can lead to a successful ATRP [38-41].

ARGET ATRP can tolerate a large excess of reducing agent and therefore should be more appropriate for systems in which air must be scavenged. This system may be particularly well-suited for grafting from large wafers because it is difficult to place them inside Schlenk flasks and carry out deoxygenation.

In the present work, we focus on the fabrication of novel nanocomposites of Silica grafted with poly(methyl methacrylate) (PMMA) via surface-initiated ARGET ATRP. The aim is to solve some problems in preparing SiO_2/PMMA composites. The great polarity difference between SiO_2 filler and PMMA matrix leads to the poor interfacial adhesion. SiO_2 nanoparticles tend to form large micro-scale aggregates and the release of SiO_2 nanoparticles from porous PMMA could cause effects such as embolism or other adverse effects. Surface modification of SiO_2 by grafting PMMA can avoid the agglomeration of SiO_2 particles and improve their compatibility with PMMA, and the entanglements between them could reduce the release of SiO_2 from PMMA matrix. The ARGET ATRP process contains two steps: introduction of initiator groups and polymerization of methyl methacrylate (MMA) on the surface of SiO_2 particles. The amount of grafted PMMA could be controlled via controlling of polymerization time. The coating PMMA improved the dispersibility and hydrophobicity of SiO_2 particles.

2.2. Experimental section

2.2.1. Materials

Silica nanopowder (15 nm) was purchased from Aldrich. 2-bromoisobutyryl bromide (2-BBB) (Aldrich) was distilled over calcium hydride (CaH_2) under reduced pressure. Triethyl amine (TEA) was purified by double distillation over p-toluenesulfonyl chloride and CaH_2, respectively. Methyl methacrylate (MMA) (99.5%, Junsei) was passed through an activated alumina column to remove the inhibitor. Copper (II) bromide (99.999%, Aldrich); *N*,*N*,*N*′,*N*″,*N*″-Pentamethyldiethylenetriamine (PMDETA) (99%, Aldrich); tin (II) 2-ethylhexanoate (95%, Aldrich); 3-aminopropyl trimethoxysilane (3-APTMS) (98%, Aldrich) and other solvent (reaction grade) were used as received without any further purification.

2.2.2. Synthesis of initiator-functionalized SiO_2 particles

The synthesis of 2-bromo-2-methyl-N-3-[(trimethoxysilyl)propyl]-propan-amide (BrTMSPA) was carried out followed the procedure in literature [42]. Namely, 3-APTMS (1.79 g, 10 mmol) was mixed with triethylamine (1.01 g, 10 mmol) in 50 mL of dried tetrahydrofurane (THF). 2-BBB (3.45 g, 15 mmol) was added dropwise into the solution for 30 min with stirring. The reaction was kept for 12 h with stirring and under nitrogen protection. The precipitate was filtered off using a frit funnel. The product was yellowish oil after the removal of the solvent. The product was re-dissolved with CH_2Cl_2 (20 mL) and washed with 0.01 N HCl (2x20 mL) and cold water (2x20 mL), respectively. The organic phase was dried with anhydrous $CaCl_2$. After the removal of the solvent, the final product was colorless oil with a yield of 92.5%. 1 H NMR (400 MHz, $CDCl_3$): δ 6.84 (s, 1H, NH), 3.55 (s, 9H, SiOC**H**$_3$), 3.24 (t, 2H, C**H**$_2$N), 1.92 (s, 6H, C**H**$_3$,), 1.63 (m, C**H**$_2$, 2H), 0.64 (t, 2H, SiC**H**$_2$).

The SiO_2 nanopowder (1.00 g) and BrTMSPA (0.50 g) were dispersed into toluene (50 mL). The mixture was stirred for 72 h at room temperature under the protection of nitrogen flow. SiO_2-Br nanoparticles were obtained by centrifugation and washed thoroughly by five centrifugation-redispersion cycles with toluene as a solvent. Finally, the product was dried until constant weight under vacuum at 45^{o}C.

2.2.3. Surface-initiated polymerization of SiO_2 macro-initiator

SiO_2-Br particles (0.500 g), PMDETA (8.6mg), $CuBr_2$ (1.11mg), MMA (5.00 g) and anisole (4mL) were added to an open-capped vial equipped with a magnetic stir bar. The SiO_2-Br particles were stirred and ultrasonicated for 30min. The system was degassed by nitrogen bubbling for 15

minutes. To this solution, a mixture of Sn(Oct)2 in 1 ml anisole was injected rapidly. The polymerization was stopped by exposing the reaction solution to air. The products were then diluted with THF, and collected by centrifugation with THF four times and methanol twice sequentially. The PMMA grafted SiO_2 nanocomposites (PMMA-g-SiO_2) were dried in vacuum at room temperature for 24h. Three separate experiments with interval reaction time were conducted in order to study the kinetic of polymerization process.

To evaluate the dependence of number–averaged molecular weight (Mn) and polydispersity index (PDI=Mw/Mn) values of the grafted PMMA on polymerization time, the PMMA chains were cleaved from the SiO_2 surface as follows: 50 mg of the PMMA-g-SiO_2 particles and 50 mg of TOAB were dissolved in 5 mL of toluene in a polyethylene flask. A 5% HF aqueous solution was then added to the mixture. The mixture was stirred vigorously for 24 h. The cleaved PMMA in the organic layer was precipitated in cold ethyl ether.

2.2.4. Characterization

Transmission Electron Microscopy (TEM) images were recorded using a Hitachi H-7500 instrument operated at 80 kV. A drop of the sample dispersed in distilled toluene was placed on a copper grid and drying. The changes in the surface chemical bonding of functionalized SiO_2 nanoparticles, SiO_2-Br, and PMMA-g-SiO_2 hybrid particles were captured by Fourier Transformed Infrared Spectrophotometry (FT-IR) using a BOMEM Hartman & Braun FT-IR Spectrometer in the frequency range of 4000-400 cm^{-1} . The morphology of the hybrids was carried out by using Field Emission Scanning Electron Microscopy (FE-SEM) images (Hitachi JEOL-JSM-6700F system, Japan). Thermogravimetric analysis (TGA) was conducted with Perkin-Elmer Pyris 1 analyzer (USA). Before the test, all the samples were carefully grinded into fine powder. The samples were scanned within the temperature range of 50–800^oC at a heating rate of 10^o $C.min^{-1}$ under continuous nitrogen flow. Surface composition was investigated using X-ray Photoelectron Spectroscopy (XPS) (Thermo VG Multilab 2000) in ultrahigh vacuum with Al Kαradiation. GPC was performed using an Agilent 1200 Series equipped with PLgel 5µm MIXED-C columns, with THF as the solvent at 30◦ C. The solution flow rate was 1 mL/min. Calibration was carried out using PMMA standards. The ^{1}H-NMR spectrum of initiator functionalized silane was recorded using a JNM-ECP 400 (JEOL) Spectrophotometer with solvent $CDCl_3$.

2.3. Result and discussion

The general approach to the preparation of PMMA grafted SiO_2 nanocomposites is illustrated in Scheme 1. First, SiO_2-Br particles were prepared by treating SiO_2 with BrTMSPA. Then surface-initiated ARGET ATRP of MMA was carried out from Br-HAP particles.

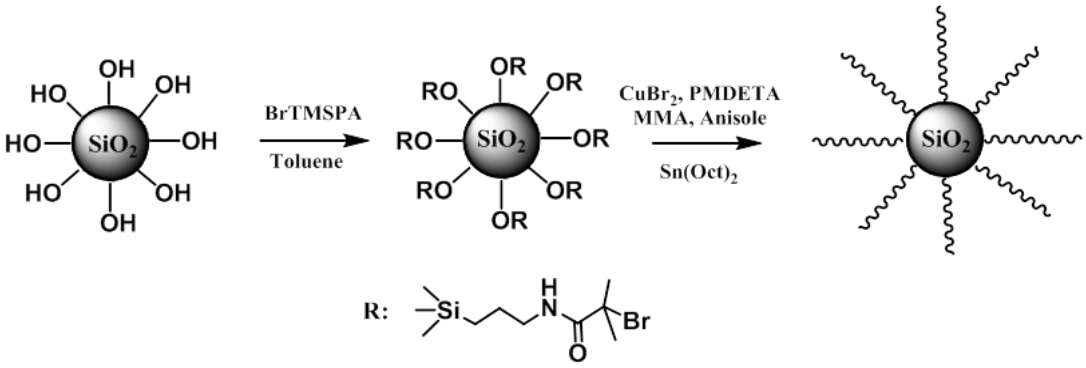

Figure 2.1. Synthetic approach for preparation of nanocomposites via surface-initiated ARGET ATRP.

Figure 2.1 shows the FTIR spectra of SiO_2 (a), SiO_2-Br (b) and PMMA-g-SiO_2 (c). For bare SiO_2 particles, the absorption peaks at 1101 cm^{-1} was responsible for stretching vibration of siloxane (Si-O-Si) group and peaks at 3414 cm^{-1} was related to free hydroxyl group stretching vibration. From Figure 2.1 (b), new adsorption peaks at 1655 cm^{-1} and 1535 cm^{-1} was assigned to the >C=O stretching vibration and N-H bending vibration. These peaks could be related to the formation of initiator layer onto silica surface. Compare to Figure 2.1 (a) and (b), the bands in the range of 3000-2850 cm^{-1} corresponding to C-H stretching vibrations of the CH_3 and CH_2 groups of grafted PMMA were recorded. In addition, a very strong peak of carbonyl group (>C=O) in the polymer backbone at 1734 cm^{-1} was also well observed. This could be assumed to the successful attachment of polymer chain onto silica surface by covalent bonds.

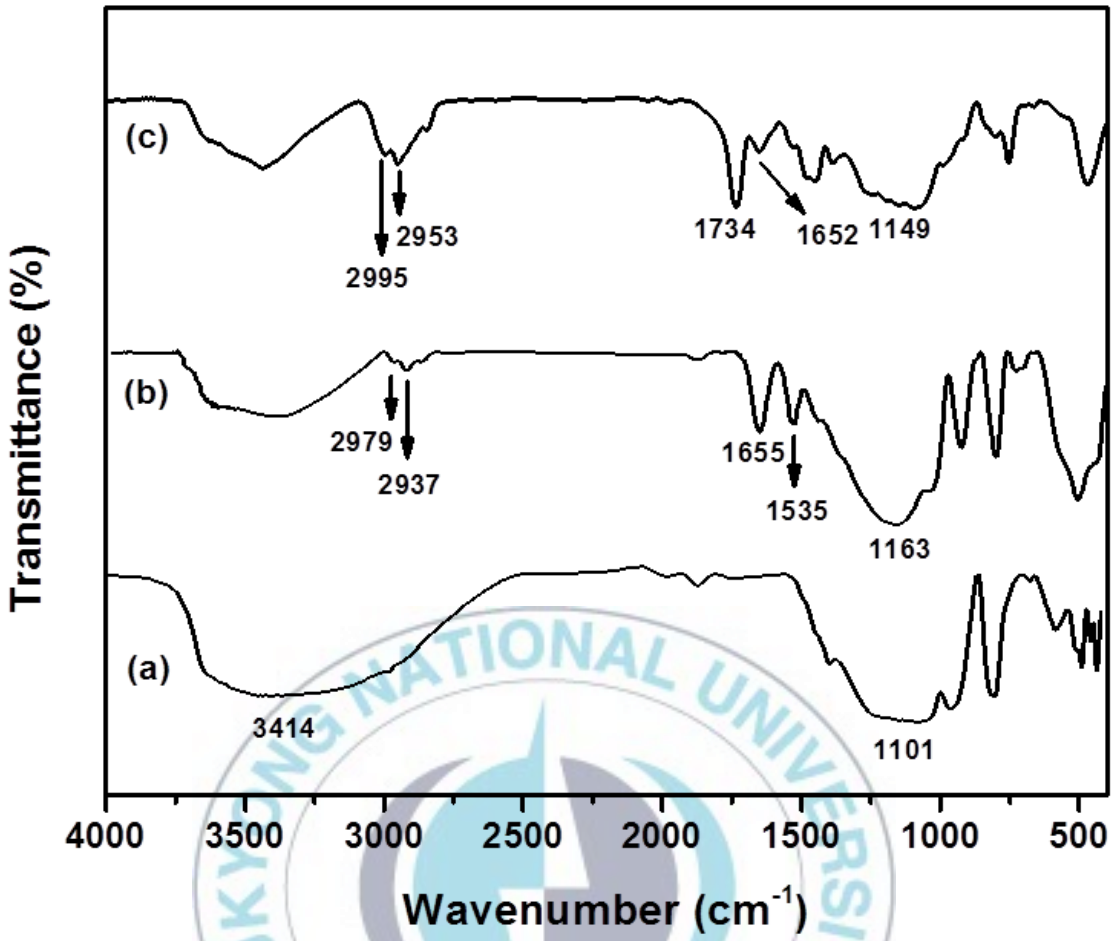

Figure 2.2. FT-IR spectra of bare SiO_2 (a), SiO_2-Br (b) and PMMA-g-SiO_2 (b).

XPS measurements were performed to investigate the surface composition of nanocomposites, as shown in Figure 2.2. The wide scan XPS spectra over a large energy range at a low resolution were measured to identify the elements present in grafted hybrid nanoparticles. In Figure 2.2 (a), the sharp peaks at 285.16, 400.47 and 70.64 eV are assigned to C1s, N1s and Br3d, respectively, in the nanoparticles, indicating the successful immobilization of ATRP initiator on the inorganic SiO_2. Upon the surface-initiated polymerization, the C1s intensity had increased significantly, Figure 2.2 (c), due to the formation of polymer chains surrounding the SiO_2 nanofillers.

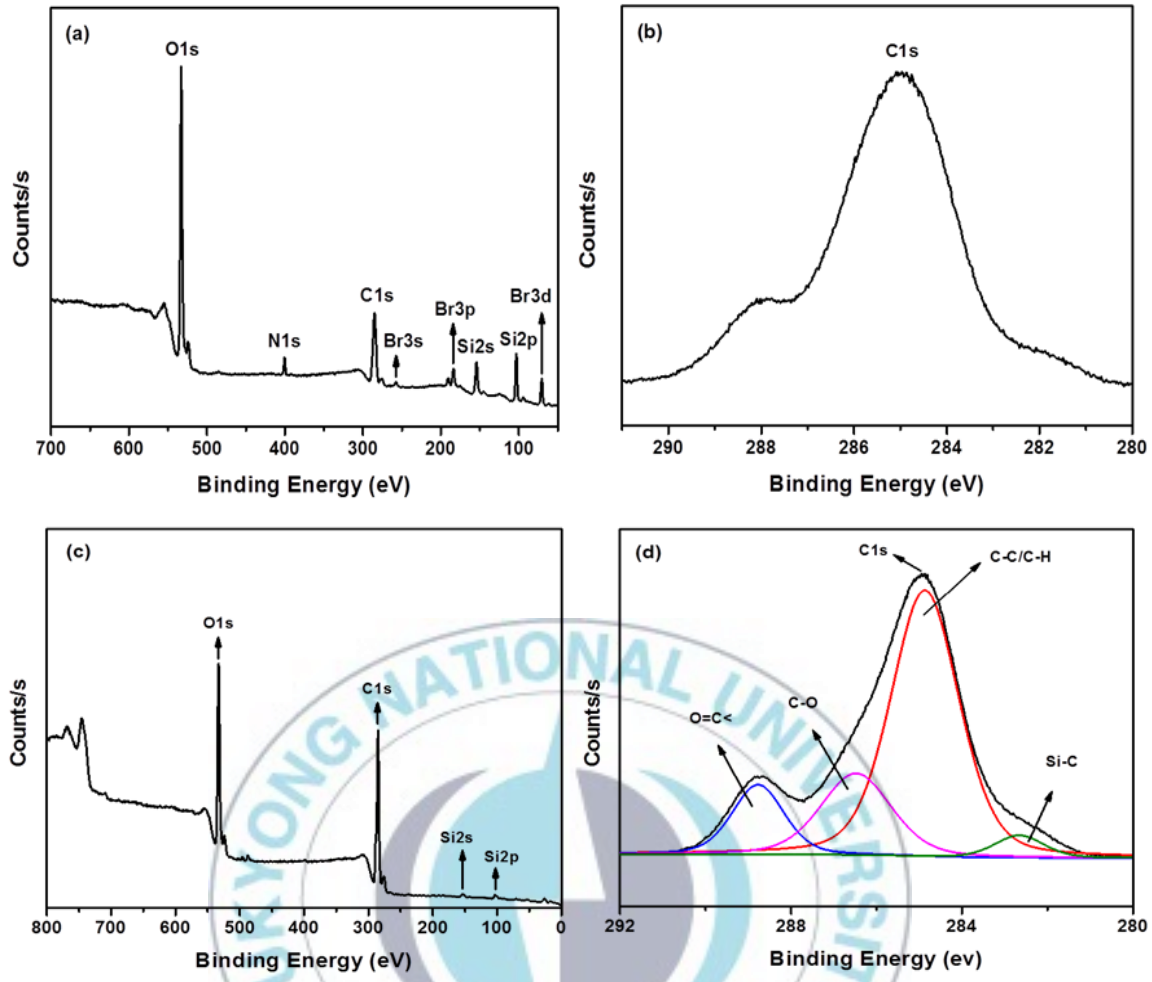

Figure 2.3. XPS wide scan spectra of SiO_2-Br (a) and PMMA-g-SiO_2 (c); XPS narrow scan spectra of SiO_2-Br (b) and PMMA-g-SiO_2 (d).

The C1s regions of the narrow scan XPS spectra for materials are very sensitive to the chemical environment surrounding the element and thus can provide important information on obtaining the strength of the interaction between the SiO_2 and the polymer chains. Figure 2.2 (d) shows the C1s region of narrow scan XPS spectra for the nanoparticles. For the grafted nanoparticles, the binding states of C1s can be deconvoluted into four contribu-tions, which corresponded to the C-H/C-C species, Si-C species, the >C=O species and the O-C species in the polymer backbone.

The PMMA-grafted SiO_2 were subjected to thermogravimetric analysis. The result from the thermogravimetric analysis of MNs is shown in Figure 2.3. The initial weight loss observed, in the vicinity of 150^{o}C, is due to the continued loss of water [43]. The SiO_2 were analyzed by thermogravimetric analysis following the anchoring of the ATRP initiator the result of which is

shown in Figure 2.3 (b). The weight loss at around 200°C (T_{onset}) corresponds to the ATRP-initiator anchored on silica nanoparticles.

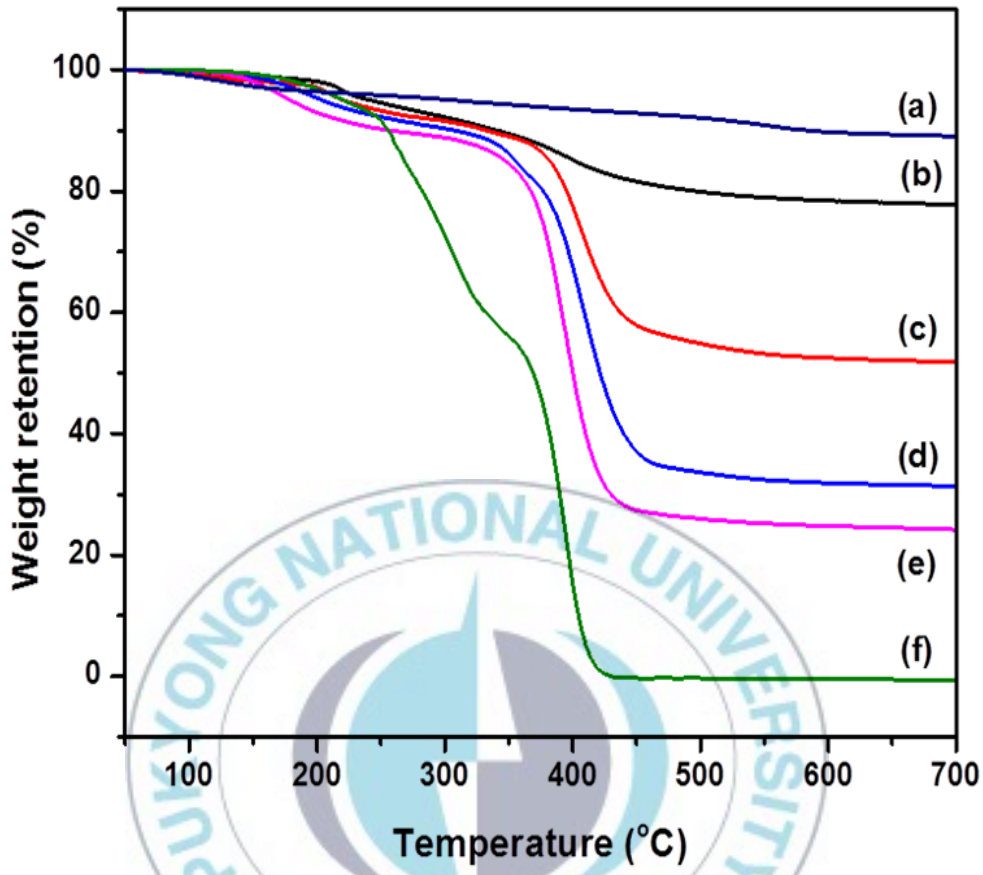

Figure 2.4. TGA curves of bare SiO_2 (a), SiO_2-Br (b), PMMA-g-SiO_2 after 6h (c), 12h (d), 24h (e) and cleaved homopolymer (f).

For the polymer-grafted SiO_2, three main weight-loss regions are observed in thermogravimetric analysis, as shown in Figure 2.3 (c), (d), and (e). The first weight-loss at 200°C can be assigned to the decomposition of initiator moiety on the surface of silica. The subsequent rapid weight decrease in the second region (the onset at 200°C) and the significant weight reduction in the third region (the onset at 360°C) are attributed to the decomposition of PMMA. The grafting amount of polymer on reaction time was estimated to be 28% for 6h, 48% for 12h and 60% for 24h.

To obtain the molecular weight details (M_n and PDI) of the grafted PMMA, the polymer chain was cleaved from the surface of SiO_2 nanoparticles by HF treatment and subjected to GPC analysis. Table 2.1 summarized GPC data for different polymerization time increased from 6 h to 24 h, the M_n of the grafted PMMA chains ranged from 22500 to 50100 with a relatively narrow PDI about

1.30 and 1.45. The narrow PDI of cleaved polymer indicated that the polymer chain was growth from silica surface with controlled manner.

Table 2.1. Molecular weight and PDI of cleaved polymer

Sample	Reaction time	Molecular weight (g/mol)	PDI (Mw/Mn)
1	6h	22500	1.45
2	12h	40600	1.39
3	24h	50100	1.30

The morphology of silica-based initiators and the resulting polymer decorated nanoparticles in the solid state were analyzed using HR-TEM. Dilute solutions of initiator-modified silica nanoparticles and PMMA-g-SiO2 nanoparticles in a good solvent toluene were cast onto carbon coated grids and analyzed after evaporation of the solvent. Figure 2.4 (a), represented the discrete nature of SiO_2 nanoparticles after the treatment with ATRP initiator functionalized silane. The TEM image of Figure 2.4 (b) reveals a polymer shell encapsulating a dense silica core, giving rise to a distinctive encapsulated hybrid nanostructure. This result was further confirmed using SEM as shown in Figure 2.4 (c) and (d). The surface morphology of the PMMA-g-SiO_2 nanopowder in the FESEM image of Figure 2.4 (d) suggests the narrowly dispersed nanoparticles were covered with an amorphous polymer layer. The increase in size of the nanocomposites from that of the silica nanospheres is readily discernible from the TEM and FE-SEM images under the same magnification.

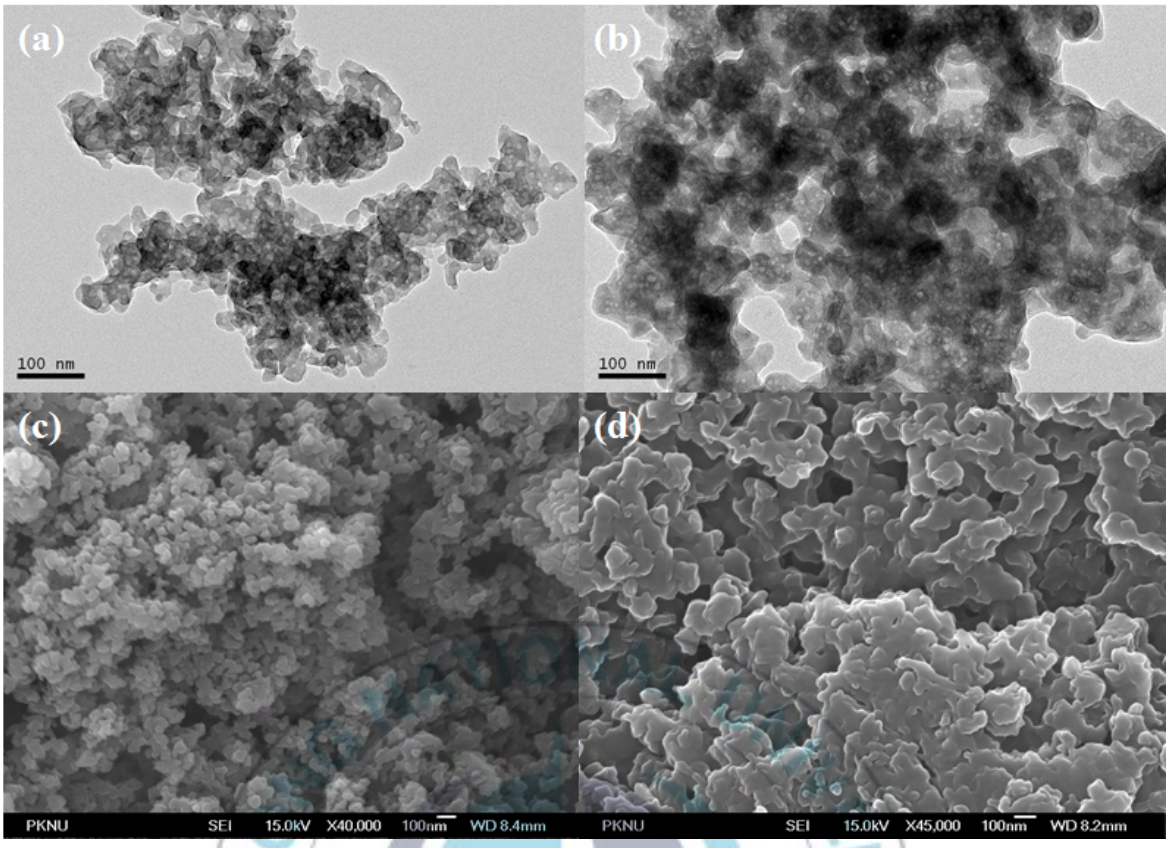

Figure 2.5. TEM images of SiO_2-Br (a) and SiO2/PMMA nanocomposites (b); FE-SEM images of SiO_2-Br (c) and SiO2/PMMA nanocomposites (d).

The silica nanoparticles were suspended in toluene before and after the grafting of the PMMA brush to study the effect on their dispersion. The photographs of SiO_2 and SiO_2 with the PMMA brush dispersed in toluene are shown in Figure 2.5 (a). The picture on the left is related to bare SiO_2 which settles down rather quickly. The extant picture is after the grafting of PMMA to SiO_2. It can be seen that a good dispersion is formed as a result of the growth of polymer chains from silica surface. The photographs of SiO_2 and SiO_2 modified with PMMA after one day of observation time were shown in Figure 2.5 (b). It can be seen that the PMMA brush does introduce reasonable long time stability to the dispersion of silica nanoparticles. Thus poly(methyl methacrylate) grafted on to the surface of SiO_2 nanoparticles was expected to enable the dispersion of particles in various organic solvents like THF, DCM and chloroform.

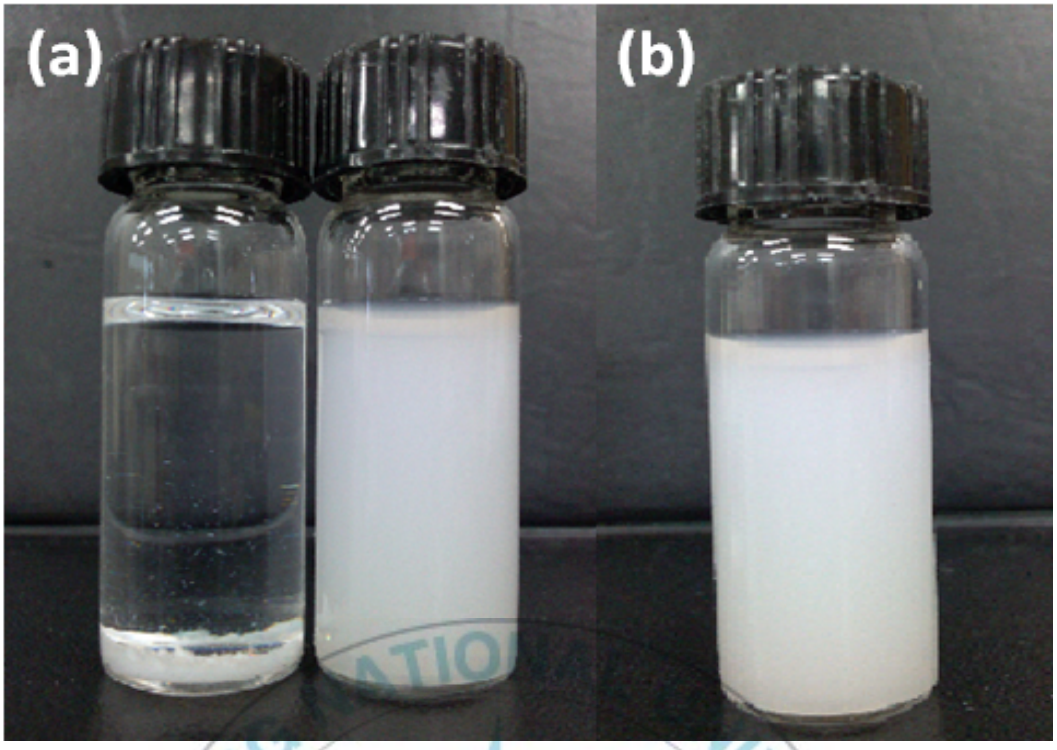

Figure 2.6. Digital photographs of bare SiO2, PMMA-g-SiO2 dispersed in toluene at preparation (a) and PMMA-g-SiO2 dispersed in toluene after 1 day (b).

2.4. Conclusion

A facile and efficient method to prepare SiO2-PMMA nanocomposites via surface-initiated ARGET ATRP has been reported. This study demonstrated that the polymerization can be conducted in a well-controlled manner in room temperature using PMDETA/ $CuBr_2$ as the catalytic system, with $Sn(Oct)_2$ as reducing agent. Above all, this versatile approach can be applied to graft other polymers with increasing complexity and functionality in the polymeric shells, and may pave the way for the design, fabrication, optimization, and eventual application of more functional SiO_2-based nanocomposites. In addition, this method is also expected for the fabrication of various polymer-inorganic nanocomposites with desired structure and properties.

2.5. References

1. H. Zou, S. Wu, and J. Shen, *Chemical Reviews* 108, 3893 **(2008)**.

2. Y. C. Ke and P. Stroeve, *Chapter 1 - Background on Polymer-Layered Silicate and Silica Nanocomposites*, in *Polymer-Layered Silicate and Silica Nanocomposites*, Elsevier Science: Amsterdam **(2005)**.

3. M. J. Tommalieh, A. M. Zihlif, and G. Ragosta, *Journal of Experimental Nanoscience* 6, 652 **(2011)**.

4. R. Scotti, L. Wahba, M. Crippa, *Soft Matter* 8, 2131 **(2012)**.

5. X. Tan, Y. Xu, N. Cai, *Polymer Composites* 30, 835 **(2009)**.

6. D. Bracho, V. N. Dougnac, H. Palza, *Journal of Nanomaterials* 2012, 8 **(2012)**.

7. R. K. Donato, K. Z. Donato, H. S. Schrekker, *Journal of Materials Chemistry* 22, 9939 **(2012)**.

8. S. Dinkar, A. Dhanabalan, and B. H. S. Thimmappa, *Journal of Applied Polymer Science* 126, 1585 **(2012)**.

9. H. Mohammad-Beigi, S. Yaghmaei, R. Roostaazad, *Physica E: Low-dimensional Systems and Nanostructures* 44, 618 **(2011)**.

10. B. Yan and Y.-F. Shao, *Dalton Transactions* **(2013)**.

11. S. M. Alahmadi, S. Mohamad, and M. J. Maah, *International Journal of Molecular Sciences* 13, 13726 **(2012)**.

12. M. Joubert, C. Delaite, E. Bourgeat Lami, *New Journal of Chemistry* 29, 1601 **(2005)**.

13. L. Basilissi, G. Di Silvestro, H. Farina, *Journal of Applied Polymer Science* 128, 3057 **(2013)**.

14. E. Kontou, M. Niaounakis, and P. Georgiopoulos, *Journal of Applied Polymer Science* 122, 1519 **(2011)**.

15. B. Lepoittevin, M. Devalckenaere, N. Pantoustier, *Polymer* 43, 4017 **(2002)**.

16. P. Hajji, L. David, J. F. Gerard, *Journal of Polymer Science Part B: Polymer Physics* 37, 3172 **(1999)**.

17. Y. Ou, F. Yang, and Z.-Z. Yu, *Journal of Polymer Science Part B: Polymer Physics* 36, 789 **(1998)**.

18. D. Fragiadakis, P. Pissis, and L. Bokobza, *Polymer* 46, 6001 **(2005)**.

19. W. A. Braunecker and K. Matyjaszewski, *Progress in Polymer Science* 32, 93 **(2007)**.

20. J.-F. Lutz, D. Neugebauer, and K. Matyjaszewski, *Journal of the American Chemical Society* 125, 6986 **(2003)**.

21. C. J. Hawker, *Journal of the American Chemical Society* 116, 11185 **(1994)**.

22. J.-S. Wang and K. Matyjaszewski, *Journal of the American Chemical Society* 117, 5614 **(1995)**.

23. R. T. A. Mayadunne, E. Rizzardo, J. Chiefari, *Macromolecules* 32, 6977 **(1999)**.

24. J. Pyun and K. Matyjaszewski, *Chemistry of Materials* 13, 3436 **(2001)**.

25. M. F. Cunningham, *Progress in Polymer Science* 33, 365 **(2008)**.

26. L. Tao, G. Mantovani, F. Lecolley, *Journal of the American Chemical Society* 126, 13220 **(2004)**.

27. Y. Tsujii, K. Ohno, S. Yamamoto, *Structure and Properties of High-Density Polymer Brushes Prepared by Surface-Initiated Living Radical Polymerization*, in *Surface-Initiated Polymerization I*, R. Jordan, Editor, Springer Berlin Heidelberg **(2006)**.

28. *Controlled Radical Polymerization*. ACS Symposium Series. Vol. 685. American Chemical Society. 500 **(1998)**.

29. K. Matyjaszewski and J. Spanswick, *Materials Today* 8, 26 **(2005)**.

30. K. Matyjaszewski, J.-L. Wang, T. Grimaud, *Macromolecules* 31, 1527 **(1998)**.

31. D. Baskaran, J. W. Mays, and M. S. Bratcher, *Angewandte Chemie International Edition* 43, 2138 **(2004)**.

32. S. Edmondson, V. L. Osborne, and W. T. S. Huck, *Chemical Society Reviews* 33, 14 **(2004)**.

33. K. Ohno, T. Morinaga, K. Koh, *Macromolecules* 38, 2137 **(2005)**.

34. S. H. Lee, D. R. Dreyer, J. An, *Macromolecular Rapid Communications* 31, 281 **(2010)**.

35. K. Min, W. Jakubowski, and K. Matyjaszewski, *Macromolecular Rapid Communications* 27, 594 **(2006)**.

36. J. K. Oh, K. Min, and K. Matyjaszewski, *Macromolecules* 39, 3161 **(2006)**.

37. J. K. Oh, H. Dong, R. Zhang, *Journal of Polymer Science Part A: Polymer Chemistry* 45, 4764 **(2007)**.

38. K. Matyjaszewski, H. Dong, W. Jakubowski, *Langmuir* 23, 4528 **(2007)**.

39. W. Jakubowski, B. Kirci-Denizli, R. R. Gil, *Macromolecular Chemistry and Physics* 209, 32 **(2008)**.

40. W. Jakubowski and K. Matyjaszewski, *Angewandte Chemie* 118, 4594 **(2006)**.

41. N. Chan, M. F. Cunningham, and R. A. Hutchinson, *Macromolecular Chemistry and Physics* 209, 1797 **(2008)**.

42. Z. Zhang, T. Chao, S. Chen, *Langmuir* 22, 10072 **(2006)**.

43. T. von Werne and T. E. Patten, *Journal of the American Chemical Society* 123, 7497 **(2001)**.

Chapter 3

A facile route for the covalent functionalization of SiO_2 nanoparticles with thermoresponsive PNIPAm employing thiol-ene chemistry and ARGET ATRP technique

Covalent functionalization of thiol-modified SiO_2 with well-defined, alkene-terminated poly(N-isopropyl acrylamide) was accomplished by the thiol-ene radical addition. The alkene-terminated ATRP initiator was first synthesized, and then the alkene-terminated thermo-responsive poly(N-isopropyl acrylamide) (PNIPAM) was synthesized by the fascinating ARGET ATRP of NIPAM monomer. The number-average molecular weights (Mn) and polydispersities (Mw/Mn) were investigated by GPC analysis. A thiol-ene based “grafting to” method was used to attach thermo-responsive polymers onto the exterior surface of SiO_2 nanoparticles which produced relatively high grafting density. The as-synthesized hybrid nanoparticles exhibited thermo-responsive behavior and were characterized by FTIR, XPS, TGA, DLS, and TEM.

3.1. Introduction

Over the past decay, novel routes for the integration of inorganic, organic, and polymer in nanoscale size has provided new opportunities in preparation of high performance advanced nanostructures [1-3]. The emergence of “click” chemistry, typically Huisgen 1,3-dipolar azide-alkyne cycloaddition and thiol-ene reaction, has attracted immense scientific interests due to its efficiency and the versatile applicability [4, 5]. The ease of synthesis of the alkene/alkyne and thiol/azide functionalities, coupled with tolerance to a wide variety of functional groups, stability and reaction conditions, make these coupling process highly attractive for the synthesis of complex macromolecular structures [6-8]. In addition, “click” chemistry has also greatly facilitated the post-modification of functional polymer [9, 10] and synthesis of nanocomposites [11, 12]. Recently, the combination of control radical polymerization (CRP) and click reaction has been reported to be a powerful strategy for the preparation of functional hybrid materials [9, 13, 14].

Two of the most successful CRP techniques are reversible addition fragmentation chain transfer (RAFT) and atom transfer radical polymerization (ATRP). Both techniques have been successfully applied for the synthesis of various homo-polymers as well as block copolymers [15-18]. Despite of such achievements, these methods suffer drawbacks that limit their use for the preparation of polymers to use in practical applications. RAFT employs the existence of a RAFT agent as a chain transfer agent, often a thiocarbonyl-based compound, to control the polymerization. If the RAFT agent is not cleaved from the polymer in post-polymerization, polymers produced via RAFT can be highly colored or toxic [19-21]. In ATRP, a transition metal catalyst (often a Cu(I)/(II) system) used with relatively high concentrations to control the polymerization leads to difficulties for purification process in order to yield products with high purity [22]. Additionally, conventional ATRP must be carried out in a completely deoxygenated atmosphere to avoid the catalyst poisoning [22]. Although there have been several advances in order to overcome these issues, some problems is still remained in this technique [23]. A new technology based on ‘‘activators regenerated by electron transfer atom transfer radical polymerization’’ (ARGET ATRP) which uses an excess amount of reducing agent to regenerate Cu(I) from Cu(II) to maintain an appropriate Cu(I)/(II) balance [24] was developed by Matyjazewski and his group [24]. The inclusion of this reducing agent allow to reduce the concentration of copper to part per million (ppm) levels and in most cases removal of the low levels of catalyst is achieved simply by precipitation of the polymer. Moreover, the using of excess reducing agent provide tolerance of oxygen, as a result, the polymerization can be conducted in the presence of limited amounts of air [24-27]. Therefore, the combination of “click” chemistry with

robust CRP techniques like ARGET ATRP may offer a superior route for the fabrication of well-defined inorganic/polymer nanocomposites.

Despite of several kinds of functional polymers could be utilized for synthesis of nanocomposites, stimuli-responsive polymers are preferable building blocks for nanofabrication and engineering of surface because they exhibit abrupt changes in their physicochemical properties correspond to the shift of external environment. By tailoring with these kinds of polymer, the surface behavior can be tunable under external stimuli, such as ionic strength, pH, as well as temperature and thereby the release of guest molecules from the surface can be controlled [28-30]. Among these type of polymers, poly(*N*-isopropylacrylamide) (PNIPAm) is one of the most extensively studied polymer due to its thermoresponsive properties [31]. PNIPAm is biocompatible and it exhibits a lower critical solution temperature (LCST) at ~32^{o}C that is nearby human body temperature [31]. Therefore, PNIPAm has been widely applied for biomedical applications including biosensor, tissue engineering and controlled drug delivery [31-33]. In addition, a varieties of nanocomposites based on PNIPAm and inorganic materials such as SiO_2 and magnetite nanoparticles have been synthesized and reported to be a promising candidate for drug nanocarriers [13, 28, 34-37].

This paper demonstrates a facile method for the versatile and efficient functionalization of SiO_2 nanoparticles with thermoresponsive polymer. The approach is based on tailor-made thiol-functionalized SiO_2 nanoparticles and alkene-functionalized PNIPAm brush precursors. To the best of our knowledge, this is the first example for the synthesis PNIPAm-g-SiO_2 nanocomposites via "thiol-ene" click chemistry and ARGET ATRP technique.

3.2. Experimental

3.2.1. Materials

N-isopropylacrylamide (NIPAm, Sigma-Aldrich, 97%) was purified by recrystallization with hexane. 2-Bromoisobutyrylbromide (2-BiBB, Sigma-Aldrich, 98%) was distilled under reduced pressure over CaH_2. 10-undecen-1-ol (Tokyo Chemical Industry, 98%), tetraethyl orthosilicate (TEOS, Sigma-Aldrich, 98%), 3-mercaptopropyl trimethoxysilane (MPTS, Sigma-Aldrich, 98%), *N,N,N',N',N"*-pentamethyldiethylenetriamine (PMDETA, Sigma-Aldrich, 99%), ammonia solution ($NH_3.H_2O$, Junsei, 28 wt %), copper (0) (99.9%), Irgacure 651(Sigma-Aldrich, 99%) and solvents (reaction grade) were used as received.

3.2.2. Synthesis of thiol-functionalized SiO_2 nanoparticles

SiO_2 nanospheres were prepared *via* sol-gel reaction according to the modified Stöber method [38, 39]. Namely, about 18 mL (0.040 mol) of tetraethyl orthosilicate (TEOS) was added dropwise to a mixture of absolute ethanol (300 mL), deionized water (30 mL), and 28 wt % ammonia solution (6 mL). The reaction mixture was stirred for 6 h at room temperature. Subsequently, 4 mL (8.4 mmol) of 3-mercaptopropyl trimethoxysilane (MPTS) was injected into the SiO_2 sol, and the reaction was allowed to proceed for another 18 h. After the reaction, the resulting SiO_2 nanospheres with thiol bonds on the surface were purified by three centrifugation/redispersion cycles in acetone, ethanol, and deionized water. The SiO_2 nanospheres were finally dried in a vacuum oven at room temperature overnight.

3.2.3. Synthesis of 10-Undecenyl 2-bromoisobutyrate (UniB-Br)

The vinyl-terminated ATRP initiator, UniB-Br, was synthesized according to following procedure: 10-undecen-1-ol (1.70 g, 0.01 mol) was mixed with triethylamine (1.01 g, 0.01 mol) in 50 mL of dried toluene. To this solution, a solution of BiBB (2.30 g, 0.01 mol) contained toluene (10ml) was added dropwise for 30 min with stirring. The reaction was kept for 12 h with stirring under nitrogen atmosphere. The precipitate was filtered off using a frit funnel. The product was yellowish oil after the removal of the solvent. The oily mixture was dissolved with toluene and washed with large amount of 0.01 N HCl and cold water, respectively. After dried with anhydrous $CaCl_2$, solvent was removed under reduced pressure. The product, 10-undecenyl 2-bromoisobutyrate (UniB-Br), was purified by SiO_2 column chromatography using hexane:ethylacetate (15:1) as eluent. The final product was colorless oil with a yield of 90.5%. ^{1}H NMR (400 MHz, $CDCl_3$): δ 5.80 (m, 1H, -C**H**=), 4.97 and 4.92 (m, 2H, **H**$_2$C=), 4.15 (t, 2H, -OC**H**$_2$-), 2.02 (m, 2H, =CH-C**H**$_2$-,), 1.92 (s, 2H, -C(C**H**$_3$)$_2$-), 1.66 (m, 2H, -C**H**$_2$-CH$_2$-O-), 1.26-1.37 (m, 12H, -(C**H**$_2$)$_6$CH$_2$CH$_2$-O-).

3.2.4. Synthesis of vinyl-terminated polymer by ARGET ATRP

The vinyl-terminated thermoresponsive PNIPAm was synthesized under mild condition by taking advantages of ARGET ATRP. The polymerization was performed in isopropyl alcohol (IPA), employing $CuBr_2$/PMDETA as catalyst and UniB-Br as initiator in the presence of copper powder as reducing agent at room temperature. In an actual process, a dry 25 mL vial equipped with a magnetic stirrer was charged with NIPAm (5.65 g, 0.0 1mol), IPA (4.0 mL), copper powder (50 mg) and UniB-Br (159 mg, 1 mmol). After sealing the vial with a septum and melting the mixture, the resulting solution was degassed by nitrogen bubbling. A degassed solution of $CuBr_2$ (1.11 mg, 5

μmol) and PMDETA ligand (8.65 mg, 50 μmol) in IPA (1.0 mL) was introduced into the vial to initiate the polymerization. The polymerization was stopped after 24 h by removing the septum and exposing the catalyst to air. The product mixture was diluted in dichloromethane and passed through a short alumina column to remove the catalyst, followed by precipitation against large amount of diethyl ether. Dissolution and precipitation was repeated several times until a white powder was obtained. The final product was dried thoroughly under vacuum prior to characterization (conversion: 60%). The polymer was analyzed by GPC and ^{1}H NMR.

3.2.5. Surface modification of SiO_2 nanoparticles by PNIPAm using "click" chemistry

About 0.12 g of the SiO_2-SH and 0.25 g (0.05 mmol) of vinyl-terminated PNIPAm were introduced into 10 mL of dichloromethane in a Pyrex tube. After the addition of sufficient amount of photoinitiator, the mixture was homogenized by ultrasonic treatment. The tube was sealed and degassed by nitrogen bubbling for 15 min. Then, the reaction mixture was exposed to an UV (365 nm) source and stirred for 24 h with magnetic stirring to ensure the completed conversion. The resultant PNIPAm-g-SiO_2 nanocomposites were precipitated in cold ethyl ether, and washed thoroughly with dichloromethane to remove the unreacted PNIPAm chains.

3.2.6. Characterization

Fourier-transform infrared (FT-IR) spectroscopy analysis was carried out on an Agilent FT-IR spectrophotometer. Transmission electron microscopy (TEM) images were obtained using a JEOL BTEM with an accelerating voltage of 80 kV. Surface composition of nanocomposites was investigated using an X-ray Photoelectron Spectroscopy (XPS) (Thermo VG Multilab 2000) in ultrahigh vacuum with Al Kα radiation. The molecular weight (M_n) and molecular weight distribution (PDI) of vinyl-terminated polymer prepared by ARGET ATRP were characterized by gel permeation chromatography (GPC). Gel Permeation Chromatography (GPC) analyses of the samples were carried out on an HP 1100 apparatus equipped with a set of four columns (10^5, 10^4, 10^3, 10^2 A˚: polymer standards service), THF was used as eluent solvent. Poly(methylmethacrylate) samples were used as standards to construct the calibration curve. Thermogravimetric analysis (TGA) was carried out on a thermo-gravimetric analyzer (TA Instrument, Model 2050) at a heating rate of 10^{o}C/min in nitrogen. The ^{1}H-NMR spectrum of UniB-Br initiator and polymers were measured using a JNM-ECP 400 (JEOL) Spectrophotometer with deuterated chloroform as solvent.

3.3. Result and discussion

The general strategy for the surface modification of SiO_2 NPs with well-defined thermoresponsive polymer by taking advantages of ARGET ATRP and thiol-ene "click" chemistry is presented in Figure 3.1.

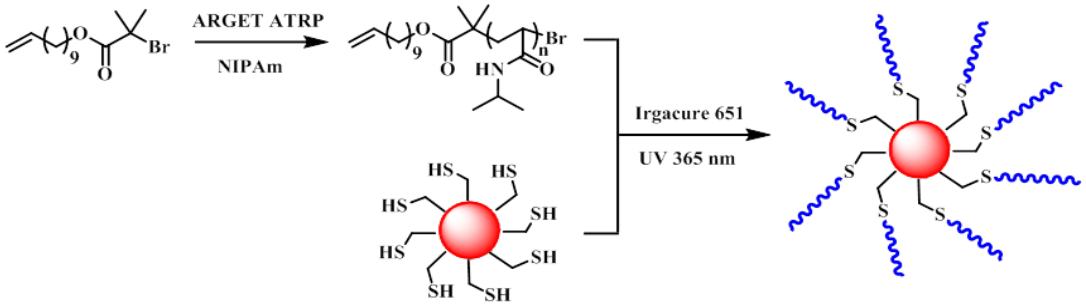

Figure 3.1. Synthetic approach for the preparation of PNIPAm-g-SiO_2 nanocomposites by the combination of click chemistry and ARGET ATRP.

In the process, firstly the preparation of thiol-functionalized SiO_2 NPs is realized. Meanwhile, vinyl-terminated polymer was prepared by a robust controlled radical polymerization. Subsequently, covalent attachment of clickable SiO_2 NPs with vinyl-terminated polymeric shells was achieved by thiol-ene chemistry.

A vinyl-terminated ATRP initiator was prepared by the esterification of alcohol and bromide acid which is widely recognized as the most efficient method for the preparation of functionalized ATRP initiator. The ^{1}H NMR spectrum of vinyl-terminated ATRP initiator is depicted in Figure 3.2 (a). ^{1}H NMR spectrum shows the peaks at (a) 5.82 and (b) 4.99 ppm, which confirmed the attachment of vinyl-terminated group to the initiator.

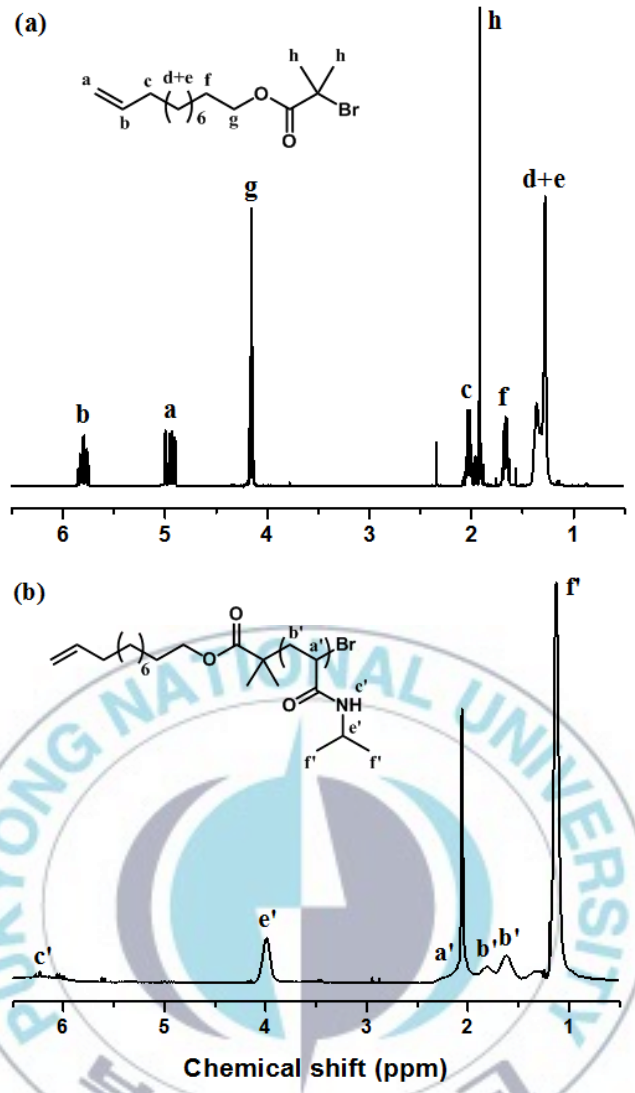

Figure 3.2. [1]H-NMR spectrum of vinyl-terminated ATRP initiator (a), and Vinyl-terminated PNIPAm (b).

By using vinyl-functionalized initiator, further modifications to attach "ene" moiety to the polymer chains are not necessary because the vinyl group of 10-undecenyl 2-bromoisobutyrate is unreactive to ATRP reaction [40]. The vinyl-terminated ATRP initiator was used for the synthesis of PNIPAm homopolymer by a facile ARGET ATRP process. Figure 3.2 (b) shows the [1]H NMR spectrum of vinyl-terminated PNIPAm. On the spectrum, characteristic signals of PNIPAm at (j) 3.98 and (k) 1.12 ppm representing methyne and methyl protons of isopropyl group are represented. In addition, the relatively broad peaks at 1.5-2.5 ppm due to the characteristic chemical shifts of polymer backbone protons are also observed. These results contributed to verify the successful synthesis of vinyl-terminated PNIPAm. From GPC analysis, the M_n and molecular weight

distribution (PDI = M_w/M_n) of the vinyl-PNIPAm were found to be 7100 g/mol and 1.21, respectively.

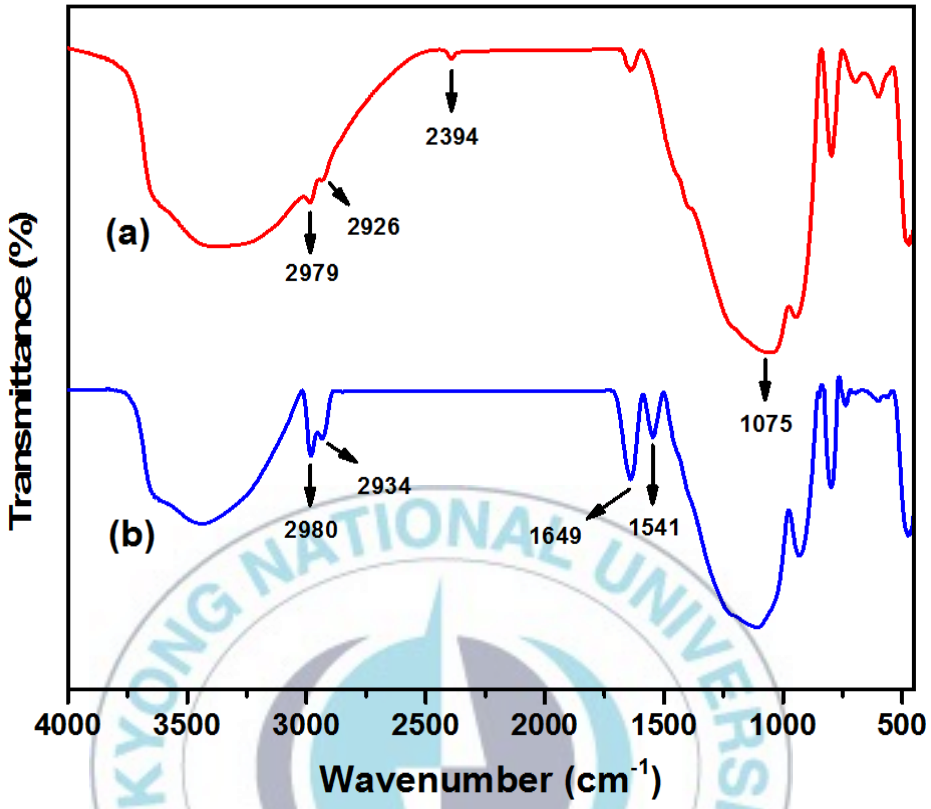

Figure 3.3. FT-IR spectrum of thiol-functionalized SiO_2 NPs (a) and PNIPAm-g-SiO_2 (b).

FT-IR was chosen because the technique is highly sensitive and it is dependable method to examine the functional groups attached to the particle surface. Figure 3.3 shows the FT-IR spectra of SiO_2-SH (a) and PNIPAm-g-SiO_2 nanoparticles (b). The FT-IR spectrum of a typical thiol-modified SiO_2 NPs is shown in Figure 3.3 (a); the weak but obvious peak at 2394 cm^{-1} corresponds to the thiol stretching vibration, whereas the peaks around 2979 to 2926 cm-1 can be attributed to the alkyl symmetric and asymmetric stretching. The thiol-functionalized SiO_2 NPs were used as the precursor materials for the ‘‘click’’ modification. After the “click” reaction, the disappearance of the thiol peak indicates successful consumption of thiol to vinyl-terminated PNIPAm through radical addition. Moreover, it can be also seen that the spectrum of PNIPAm-g-SiO_2 exhibited the strong absorption at 1649 and 2980 cm^{-1}, attributable to the stretching vibration of carbonyl group (>C=O) and polymer chain alkyl group (-CH_2, -CH_3), respectively. These FT-IR spectroscopic results confirm the successful covalent attachment of polymers onto the surface of SiO_2 NPs via “click” process.

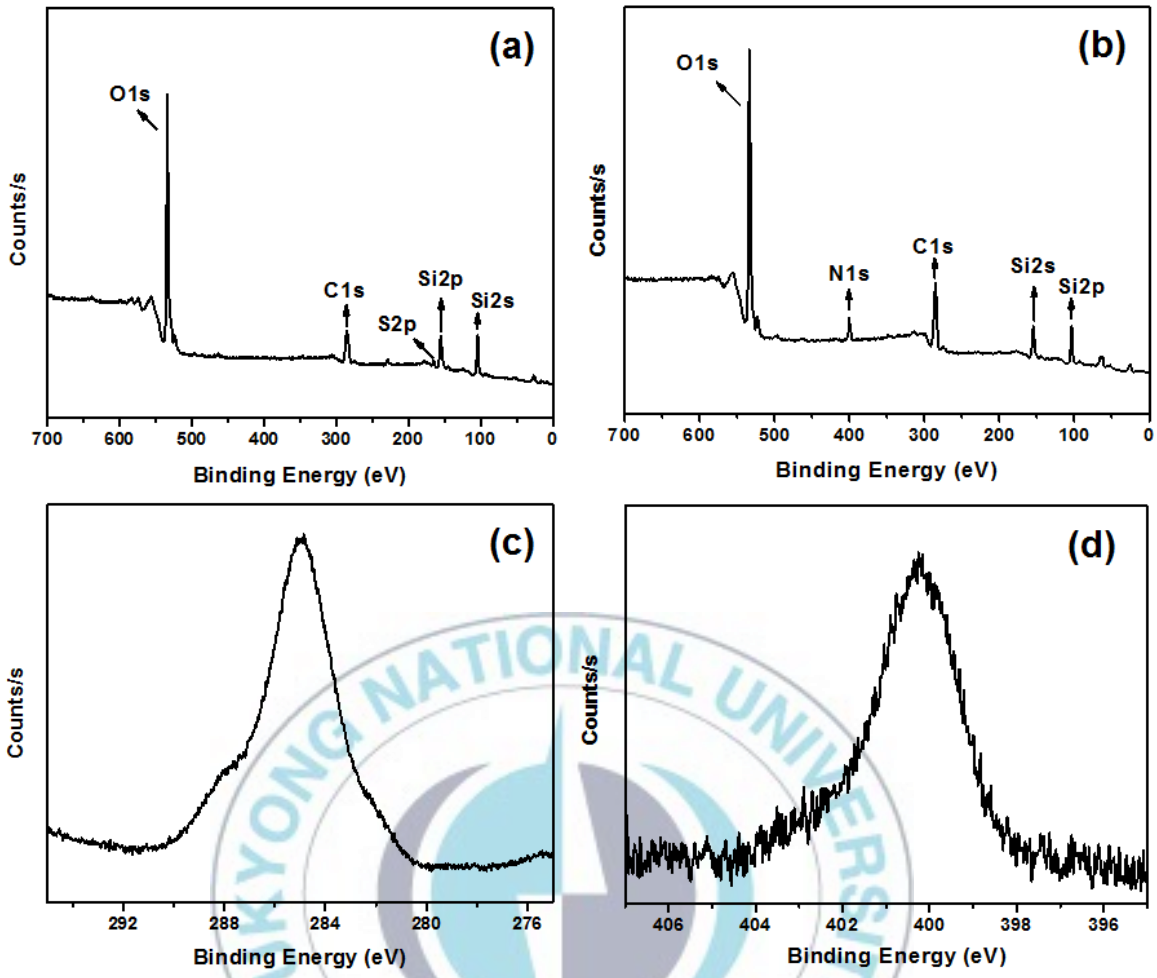

Figure 3.4. XPS (a) wide scan of the SiO_2-SH, (b) wide scan of SiO_2-PNIPAm, (c) C1s core level and (d) N1s core level of SiO_2-PNIPAm.

XPS was employed to characterize the changes in chemical composition of the nanospheres surface during the modification process. Figure 3.4 (a) and (b) present the XPS wide scan spectra of the SiO_2-SH and PNIPAm-g-SiO_2 nanocomposites, respectively. The existence of the C1s and S2p signals in SiO_2-SH spectrum was attributed to the organic composition of silane agent attached onto surface of SiO_2 NPs. By comparison from Figure 3.4 (b) to Figure 3.4 (a), the appearance of signal at 400.4 eV due to N1s indicated the success of the covalent attachment of polymer chain onto SiO_2 NPs surface upon the click modification. The subsequent thiol-ene click grafting of PNIPAm brushes on the nanospheres has also caused a remarkable increasing in intensity of the C1s signal.

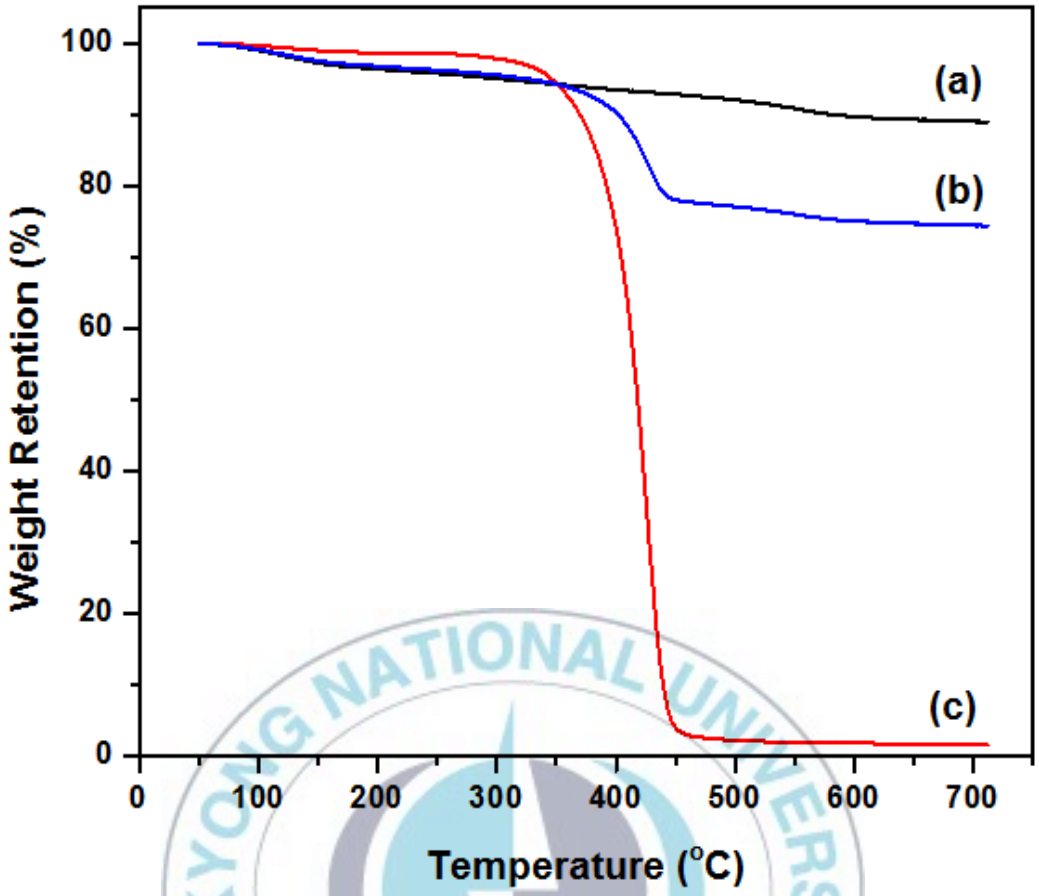

Figure 3.5. TGA curve of SiO_2-SH (a), PNIPAm-g-SiO_2 (b), and PNIPAm homopolymer (c).

The degree of functionalization of the SiO_2 NPs via "click" protocol was investigated through TGA analysis. The TGA curves of the SiO_2-SH (a), PNIPAm-g-SiO_2 (b) and PNIPAm homopolymer (c) are shown in Figure 3.5, as exhibiting the variation of residual masses of the samples depended on temperature. The major weight loss stage occurred at around 360^{o} C can be attributed to the decomposition of PNIPAm chain. Based on TGA, the content of PNIPAm in the composites can be estimated to be 18%.

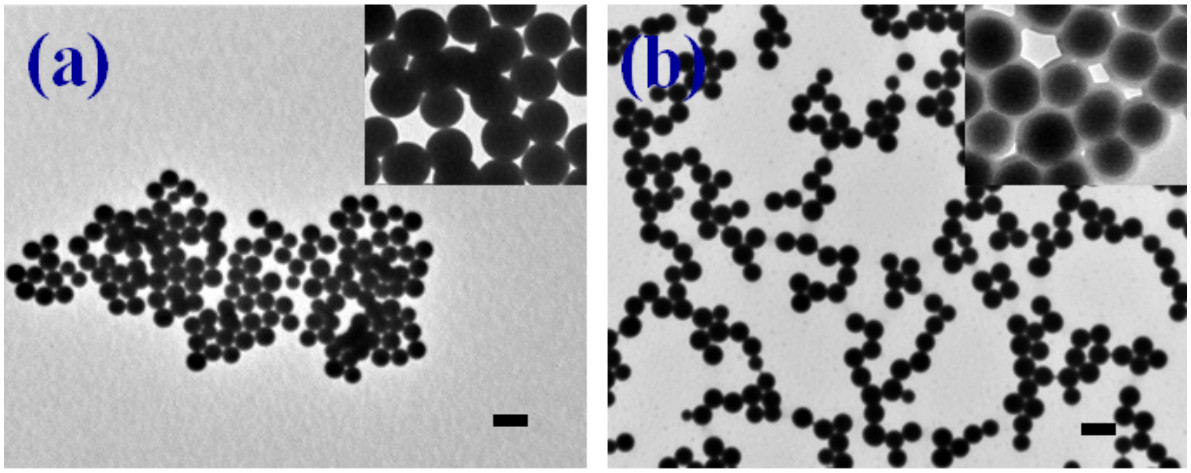

Figure 3.6. TEM micrograph of SiO_2-SH (a), and SiO_2-PNIPAm (b) (Scale bar 200 nm).

The TEM micrographs for bare SiO_2 NPs, the modified SiO_2 NPs are depicted in Figure 3.6. The samples were prepared from chloroform solution (1% wt) by drop-casting method. The SiO_2-SH NPs exhibited an average external diameter *ca.* 100 nm and showed relatively broad size distribution (Figure 3.6a). After the modification, the existence of a polymer layer which was estimated to be *ca.* 15 nm as an outer shell (lighter color) surrounding SiO_2 NPs could be clearly observed (Figure 3.6b). It can be concluded that SiO_2 NPs were successfully encapsulated by PNIPAm shells employing thiol-ene click chemistry.

The colloidal stability of SiO_2 NPs was improved significantly by the covalent PNIPAm chain functionalization. The digital photographs of SiO_2-SH and PNIPAm-g-SiO_2 nanocomposites in the chloroform are shown in Figure 3.7 for the comparative study. The as-synthesized nanocomposites exhibit good dispersion in chloroform, while SiO_2-SH showed the large aggregation. Moreover, the SiO_2-SH precipitated in chloroform within a few minutes, whereas the nanocomposites remained well dispersed in chloroform for prolonged period (Figure 3.7b). It could be deduced that the PNIPAm chain might play the role of steric stabilizing layer to prevent agglomeration resulting in superior colloidal stability.

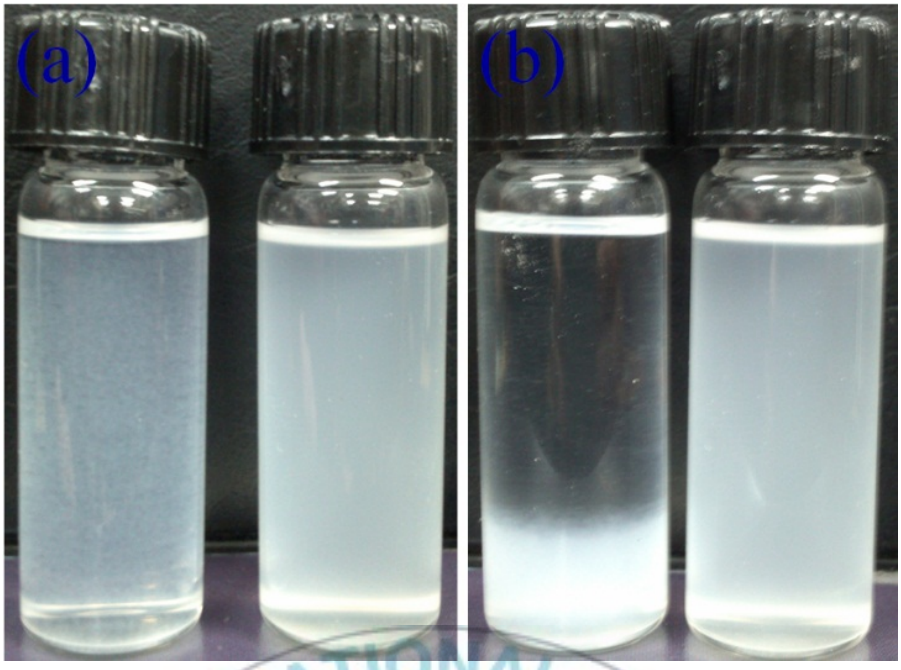

Figure 3.7. Digital photographs of SiO_2-SH and PNIPAm-g-SiO_2 dispersed in chloroform at preparation (a) and after 27 h (b).

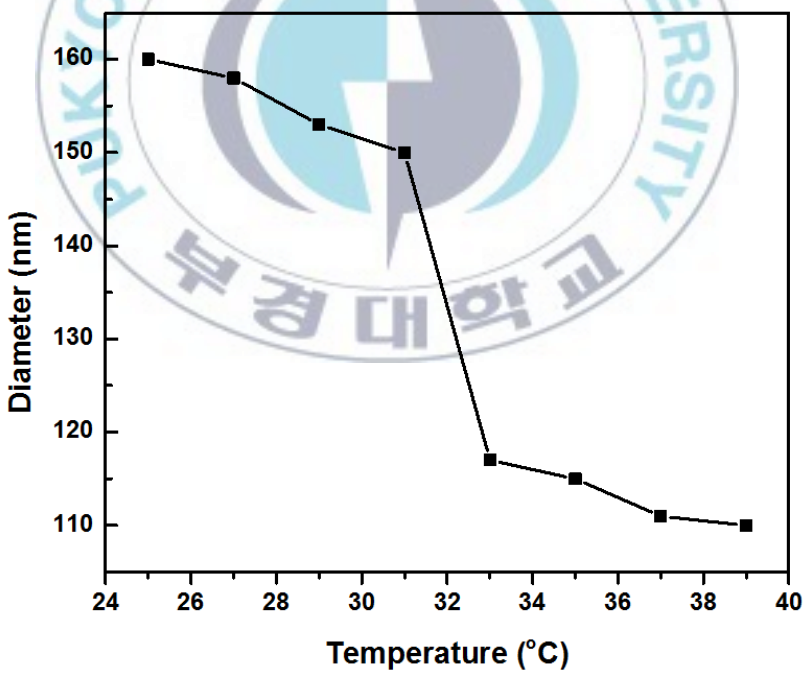

Figure 3.8. Diameter of SiO_2-PNIPAm nanocomposites in response to shift of temperature.

The thermo-responsive property of PNIPAm-g-SiO_2 nanocomposites was studied by dynamic light scattering (DLS) at a range of temperatures increasing from 25 ℃ to 39 ℃. The relationship between the hydrodynamic diameter of the nanocomposites and temperature was depicted in Figure

3.8. At the temperature from 25 ℃ to 31 ℃, PNIPAM is hydrophilic and soluble in water; the PNIPAM chains exist in a coil state, forming a solvated, incompact nanoshell on the exterior surface of SiO_2. As a result, the nanospheres diameter negligibly decreased in that range of temperature. When the temperature crossed the lower critical solution temperature (LCST), in range of 31^oC to 33^oC, the hydrodynamic diameter of the core-shell nanostructure decreased dramatically because the hydrophilic chains in water underwent the inverse phase transition state to be hydrophobic. Therefore, long PNIPAM chains collapsed toward the surface of SiO_2, forming a compact closed nanoshell around the exterior surface of SiO_2. These results suggest that the surface of SiO_2 nanoparticles has been tailored with the thermo-responsive behavior of PNIPAm by click reaction.

3.4. Conclusion

In this study, we demonstrated a robust protocol for the covalent immobilization of thermoresponsive polymer onto SiO_2 NPs core employing the combination of ARGET ATRP and click chemistry. The thiol-ene approach for grafting vinyl-terminated polymers is straightforward and effective method to directly graft polymers to the accessible thiol on surface of SiO_2 NPs in a one-step process. The success of functionalization was confirmed by surface analysis methods (FT-IR and XPS). The molecular weight and molecular weight distributions of the grafted polymer were calculated to be 7100 kg/mol and 1.21, respectively. TGA analysis revealed that the content of PNIPAm in the composites was calculated to be 15%. TEM images of the bare and modified SiO_2 NPs suggested that the SiO_2 NPs core were covered by soft polymer layer. The combination of click chemistry and ARGET ATRP to construct well-defined hybrid nanostructures with multifunctional surface is expected to allow the mimicking of more complex molecules and macromolecular structures in life science as well as for the applications in multifunctional and stimuli-responsive delivery systems.

3.5. References

1. C. K. Ober, S. Z. D. Cheng, P. T. Hammond, *Macromolecules* 42, 465 **(2008)**.
2. C. J. Hawker and K. L. Wooley, *Science* 309, 1200 **(2005)**.
3. A. B. Descalzo, R. Martínez-Máñez, F. Sancenón, *Angewandte Chemie International Edition* 45, 5924 **(2006)**.
4. A. K. Tucker-Schwartz, R. A. Farrell, and R. L. Garrell, *Journal of the American Chemical Society* 133, 11026 **(2011)**.

5. C. R. Becer, R. Hoogenboom, and U. S. Schubert, *Angewandte Chemie International Edition* 48, 4900 **(2009)**.
6. B. A. Laurent and S. M. Grayson, *Journal of the American Chemical Society* 128, 4238 **(2006)**.
7. J. N. Hoskins and S. M. Grayson, *Macromolecules* 42, 6406 **(2009)**.
8. D. M. Eugene and S. M. Grayson, *Macromolecules* 41, 5082 **(2008)**.
9. A. B. Lowe, *Polymer Chemistry* 1, 17 **(2010)**.
10. L. M. Campos, K. L. Killops, R. Sakai, *Macromolecules* 41, 7063 **(2008)**.
11. J. Amici, M. U. Kahveci, P. Allia, *Journal of Materials Science* 47, 412 **(2012)**.
12. J. Amici, P. Allia, P. Tiberto, *Macromolecular Chemistry and Physics* 212, 1629 **(2011)**.
13. J. Chen, M. Liu, C. Chen, *ACS Applied Materials & Interfaces* 3, 3215 **(2011)**.
14. S.-W. Kuo, J.-L. Hong, Y.-C. Huang, *Journal of Nanomaterials* 2012, 10 **(2012)**.
15. K. Matyjaszewski, *Macromolecules* 45, 4015 **(2012)**.
16. V. Bulmus, *Polymer Chemistry* 2, 1463 **(2011)**.
17. M. Semsarilar and S. Perrier, *Nat Chem* 2, 811 **(2010)**.
18. C. Boyer, M. H. Stenzel, and T. P. Davis, *Journal of Polymer Science Part A: Polymer Chemistry* 49, 551 **(2011)**.
19. C.-W. Chang, E. Bays, L. Tao, *Chemical Communications* 0, 3580 **(2009)**.
20. T. L. U. Nguyen, B. Farrugia, T. P. Davis, *Journal of Polymer Science Part A: Polymer Chemistry* 45, 3256 **(2007)**.
21. M. H. Stenzel, C. Barner-Kowollik, T. P. Davis, *Macromolecular Bioscience* 4, 445 **(2004)**.
22. J. Xia and K. Matyjaszewski, *Macromolecules* 32, 2434 **(1999)**.
23. N. V. Tsarevsky and K. Matyjaszewski, *Chemical Reviews* 107, 2270 **(2007)**.
24. K. Matyjaszewski, W. Jakubowski, K. Min, *Proceedings of the National Academy of Sciences* 103, 15309 **(2006)**.
25. K. Matyjaszewski, H. Dong, W. Jakubowski, *Langmuir* 23, 4528 **(2007)**.
26. N. Chan, M. F. Cunningham, and R. A. Hutchinson, *Macromolecular Chemistry and Physics* 209, 1797 **(2008)**.
27. S. M. Paterson, D. H. Brown, T. V. Chirila, *Journal of Polymer Science Part A: Polymer Chemistry* 48, 4084 **(2010)**.
28. Y.-H. Lien, T.-M. Wu, J.-H. Wu, *Journal of Nanoparticle Research* 13, 5065 **(2011)**.
29. I. Varga, I. Szalai, R. Mészaros, *The Journal of Physical Chemistry B* 110, 20297 **(2006)**.
30. A. N. Zelikin, *ACS Nano* 4, 2494 **(2010)**.

31. R. Pelton, *Advances in Colloid and Interface Science* 85, 1 **(2000)**.
32. P. Heinz, F. Brétagnol, I. Mannelli, *Journal of Physics: Conference Series* 100, 012033 **(2008)**.
33. S. Ohya, Y. Nakayama, and T. Matsuda, *Biomacromolecules* 2, 856 **(2001)**.
34. J.-H. Park, Y.-H. Lee, and S.-G. Oh, *Macromolecular Chemistry and Physics* 208, 2419 **(2007)**.
35. F. Zhang, G. Hou, S. Dai, *Colloid & Polymer Science* 290, 1341 **(2012)**.
36. K. Nagase, J. Kobayashi, A. Kikuchi, *ACS Applied Materials & Interfaces* 4, 1998 **(2012)**.
37. R. M. K. Ramanan, P. Chellamuthu, L. Tang, *Biotechnology Progress* 22, 118 **(2006)**.
38. W. Stöber, A. Fink, and E. Bohn, *Journal of Colloid and Interface Science* 26, 62 **(1968)**.
39. H. S. Hwang, J. H. Bae, H. G. Kim, *European Polymer Journal* 46, 1654 **(2010)**.
40. I. M. Ward, *Contemporary Physics* 50, 670 **(2009)**.

Acknowledgements

First of all, I would like to give the most special and sincere thanks to my supervisor Prof. Kwon Taek Lim for all his support, encouragement, guidance, patience and knowledge. Thank you for your trust, effort, times and for all the opportunities you provided me.

My acknowledgements also go to my thesis committee, Prof. Hoon Heo and Prof. Jong Tae Kim, for enthusiastic reviewing my dissertation and giving me valuable comments and suggestions. Also, I would like to make a special mention about all professors in the Department of Image System Engineering for their teaching and guidance throughout the study period.

Except for the science knowledge, the financial support also played an important role in my Master study. I would like to express my sincere gratitude to the Korea Research Foundation (KRF) and Brain Korea 21 (BK21) for financial support of this work.

I would like express my heartfelt thanks to Pukyong National University authorities and the members of the office of the international relations for their cooperation in every possible aspect.

I wish to thank all my laboratory co-workers in our research group and friends in the department for their love and support. I am also sincerely thankful to Dr Md. Rafiqul Islam, Bach Long Giang, Cao Xuan Thang and Niru for their kind support on researches, experiments and projects. During the years of study, I developed chummy friendship with them.

The last but not least, I would like to express my deepest gratitude to my parents, my brother and my cherish wife Tran Thi Nga for their selfless love and support throughout all these years. I am most grateful to my wife for giving me constant encouragement in the pursuit of my goals. Without their encouragements, I could not have completed this dissertation.